

UNCLASSIFIED

AD NUMBER
AD273744
NEW LIMITATION CHANGE
TO Approved for public release, distribution unlimited
FROM Distribution authorized to U.S. Gov't. agencies and their contractors; Administrative/Operational Use; DEC 1961. Other requests shall be referred to U.S. Army Signal Corps, Washington, DC.
AUTHORITY
USAEC ltr, 1 Dec 1972

THIS PAGE IS UNCLASSIFIED

UNCLASSIFIED

AD 273 744

*Reproduced
by the*

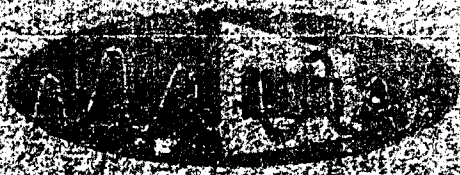
ARMED SERVICES TECHNICAL INFORMATION AGENCY
ARLINGTON HALL STATION
ARLINGTON 12, VIRGINIA



UNCLASSIFIED

NOTICE: When government or other drawings, specifications or other data are used for any purpose other than in connection with a definitely related government procurement operation, the U. S. Government thereby incurs no responsibility, nor any obligation whatsoever; and the fact that the Government may have formulated, furnished, or in any way supplied the said drawings, specifications, or other data is not to be regarded by implication or otherwise as in any manner licensing the holder or any other person or corporation, or conveying any rights or permission to manufacture, use or sell any patented invention that may in any way be related thereto.

273 744



BROADBAND RIDGE WAVEGUIDE AND
COMPONENTS

FINAL REPORT

Contract No. DA-36-019-SC-3534

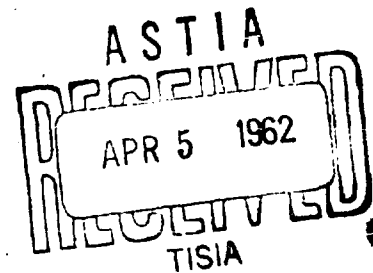
Period: July 1960 to November 1961

BROADBAND RIDGE WAVEGUIDES AND
COMPONENTS

FINAL REPORT

Contract No. DA-36-039 SC-85349

Period: 1 July 1960 to 31 November 1961



QUALIFIED REQUESTORS MAY OBTAIN COPIES OF
THIS REPORT FROM ASTIA. FOREIGN ANNOUNCE-
MENT AND DISSEMINATION OF THIS REPORT BY
ASTIA IS LIMITED

BROADBAND RIDGE WAVEGUIDES AND COMPONENTS
FINAL REPORT

Period: 1 July 1960 to 31 November 1961

OBJECTIVES:

The objectives of this contract are to design and fabricate components with double ridge cross section in the 11.0 to 26.5 frequency range.

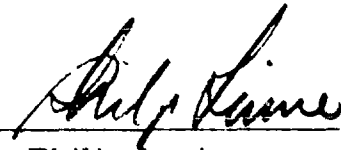
Contract No. DA-36-039 SC-85349

Signal Corps Technical Requirements No. SCL-2101K, 20 April 1959

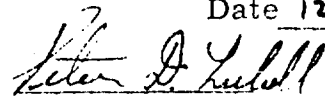
United States Army Signal Supply Agency Laboratory
Procurement Support Office

NARDA Manufacturing Corp., and
NARDA Microwave Corp. as
Joint Venturers
Plainview, L.I., New York

Authors:

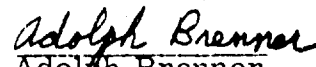

Philip Levine
Project Engineer

Date 12/11/61


Peter Lubell
Microwave Engineer

Date 12/11/61

Approved:


Adolph Brenner
Microwave Section Head

Date 12/11/61

AD

Accession No. _____

Unclassified

Narda Manufacturing and Narda Microwave Corp., Plainview, N. Y.
Broadband Ridge Waveguides and Components - P. Levine, P. Lubell,
A. Brenner

1. Broadband Microwave
Waveguide and
Components

2. Signal Corps. Contract
No. DA36-039 SC 85349

Final Report 1 July 1960 to 31 November 1961 pp-Illus-Graphs Signal
Corps Contract No. DA36-039 SC 85349, DA Task No. _____
Unclassified Report

This contract involves the design and development of microwave components in double rounded ridged waveguide for the 11.0 to 26.5 Gc frequency range. The components developed during this contract will operate over the frequency range now covered by portions of three standard rectangular waveguides, namely RG-52/U, 11.0 to 12.4 Gc; RG-91/U, 12.4 to 18.0 Gc; and RG-53/U, 18.0 to 26.5 Gc. The components developed are comparable in performance to rectangular waveguide components and may be used for test or systems application. Theoretical and empirical design procedures are discussed for the various components and their final performance data are presented.

TABLE OF CONTENTS

	<u>Page</u>
PURPOSE	1
ABSTRACT	1
FACTUAL DATA	
I. INTRODUCTION	3
II. DESCRIPTION OF COMPONENTS	11
Slotted Section	11
Adapters, Double Ridge to Rectangular	19
Sliding Termination	23
Tunable Crystal Bolometer Mount	23
Variable Attenuator	32
E-H Tuner	39
Tunable Waveguide Short	43
Rotary Joint	45a
Directional Coupler	51
Balanced Mixer	52
Flanges	70
III. CONCLUSIONS	75
IV. RECOMMENDATIONS	76
IDENTIFICATION OF KEY PERSONNEL	77
REFERENCES	78
APPENDICES	
A. RIDGE WAVEGUIDE TO RECTANGULAR WAVEGUIDE TRANSITION DESIGN PROCEDURE	A1 - A8
B. DIRECTIONAL COUPLER DESIGN PROCEDURE	B1 - B5

LIST OF ILLUSTRATIONS

<u>FIGURE</u>	<u>DESCRIPTION</u>	<u>PAGE</u>
1.	11.0 - 26.5 Gc RIDGE WAVEGUIDE CONFIGURATION	2
2.	RIDGE WAVEGUIDE EQUIVALENT CIRCUIT	2
3.	ELECTRIC FIELD STRENGTH OF ROUNDED CORNERS	4
4.	2.4:1 BANDWIDTH DOUBLE RIDGE WAVEGUIDE CHART	6
5.	POWER HANDLING CAPACITY - RIDGE AND RECTANGULAR WAVEGUIDES	7
6.	ATTENUATION - RIDGE AND RECTANGULAR WAVEGUIDES	8
7.	PHOTOGRAPH - SLIDING TERMINATION	12
8.	PHOTOGRAPH - WAVEGUIDE TRANSITIONS	13
9.	PHOTOGRAPH - ROTARY JOINT	14
10.	PHOTOGRAPH - BALANCED MIXER	15
11.	SLOTTED SECTION	17
12.	SLOTTED SECTION PROBE DETAIL	18
13.	D11-220 PRECISION SLOTTED SECTION SERIAL No. 1	20
14.	DOUBLE RIDGE TO RECTANGULAR WAVEGUIDE ADAPTER	21
15.	DOUBLE RIDGE TO RECTANGULAR WAVEGUIDE ADAPTERS, SERIAL NOS. 1 and 2 (FINAL DATA)	24
16.	SLIDING MATCHED TERMINATION	25
17.	DOUBLE RIDGE GUIDE SLIDING MATCHED TERMINATION (TYPICAL DATA)	26
18.	DOUBLE RIDGE WAVEGUIDE TUNABLE DETECTOR MOUNT ASSEMBLY	27

<u>FIGURE</u>	<u>DESCRIPTION</u>	<u>PAGE</u>
19.	DETAIL OF BOLOMETER MOUNT SHOWING DETECTOR CARTRIDGE AND WAVEGUIDE TO COAXIAL ADAPTER	28
20.	MOUNTING OF COAXIAL CARTRIDGE DETECTOR IN WAVEGUIDE	30
21.	INPUT VSWR OF D11-510 DETECTOR MOUNT	31
22.	MECHANICAL CONFIGURATION OF VARIABLE FLAP ATTENUATOR	32
23.	DOUBLE RIDGE GUIDE ATTENUATOR	33
24.	VARIABLE ATTENUATOR CONFIGURATIONS	34
25.	STEP DISCONTINUITY SUSCEPTANCE	36
26.	ATTENUATOR CALIBRATION CURVE	37
27.	VARIABLE ATTENUATOR MODEL D11-750, SERIAL No. 1, MAXIMUM VSWR, INSERTION DIFFERENT AT DIFFERENT FREQUENCIES	38
28.	E-H TUNER SHOWING JUNCTION AND ORIENTATION OF WAVEGUIDES	40
29.	E-H TUNER SHOWING CONTINUITY OF DOUBLE RIDGE IN E-PLANE	41
30.	END VIEW OF E-H TUNER SHOWING H-ARM COUPLING	42
31.	TUNABLE WAVEGUIDE SHORT	44
32.	BROADBAND CHARACTERISTICS OF D11-310 MOVEABLE SHORT CIRCUIT	45
33.	DOUBLE RIDGE GUIDE ROTARY JOINT	46
34.	CENTER CONDUCTOR BEARING CONFIGURATIONS	48
35.	D11 2274 DOUBLE RIDGE ROTARY JOINT SERIAL No. 1	49
36.	RIDGE GUIDE - DIRECTIONAL COUPLER CONFIGURATIONS	51
37.	COUPLING vs. HOLE DIAMETER FOR DIRECTIONAL COUPLER	53

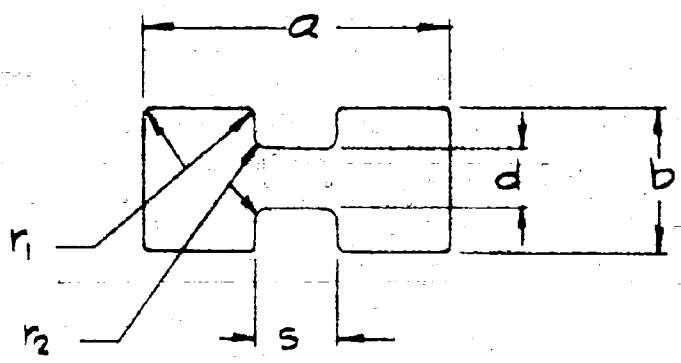
<u>FIGURE</u>	<u>DESCRIPTION</u>	<u>PAGE</u>
38	D11-1070-20 DIRECTIONAL COUPLER (FINAL DATA)	54
39	PHASE RELATIONS IN THE 90° MIXER	56
40	SKETCH OF SIDEWALL COUPLED RIDGE GUIDE COUPLER USING WIRE GRATING	59
41	SCHEMATIC REPRESENTATION OF RE- VERSED FIELD MIXER	61
42	COUPLING SECTION OF REVERSED PHASE MIXER SHOWING SIGNAL AND L.O. POWER SPLITTERS	63
43	ELECTRIC FIELD CONFIGURATIONS FOR RIDGE GUIDE STRUCTURES	64
44	SIMPLIFIED SKETCH OF CRYSTAL MOUNT for D11- BALANCED MIXER	66
45	COMPENSATION FOR SEPTUM DISCONTINUITY	68
46	DOUBLE RIDGE GUIDE FLANGE	71
47	MINIATURE UNPRESSURIZED CONTACT FLANGE FOR DOUBLE RIDGE WAVEGUIDE	72
48	MINIATURE UNPRESSURIZED CONTACT FLANGE FOR DOUBLE RIDGE WAVEGUIDE	73
49	FLANGE CHART	74

PURPOSE:

The goal of this contract is the design and development of workable components for test and systems use in double rounded ridge waveguide for the 11.0 to 26.5 Gc frequency range.

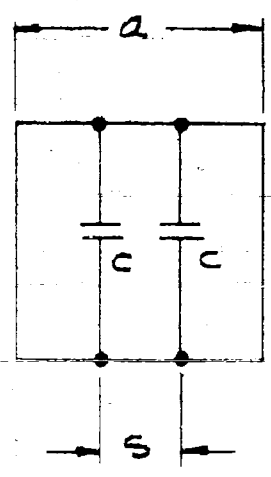
ABSTRACT:

This contract involves the design and development of microwave components in double rounded ridge waveguide for the 11.0 to 26.5 frequency range. The components developed during this contract will operate over the frequency range now covered by portions of three standard rectangular waveguides namely RG-52/U, 11.0 to 12.4 Gc; RG-91/U, 12.4 to 18 Gc; and RG-53/U, 18 to 26.5 Gc. The components developed are comparable in performance to rectangular waveguide components and may be used for test or systems application. Theoretical and empirical design procedures are discussed for the various components and their final performance data is given.



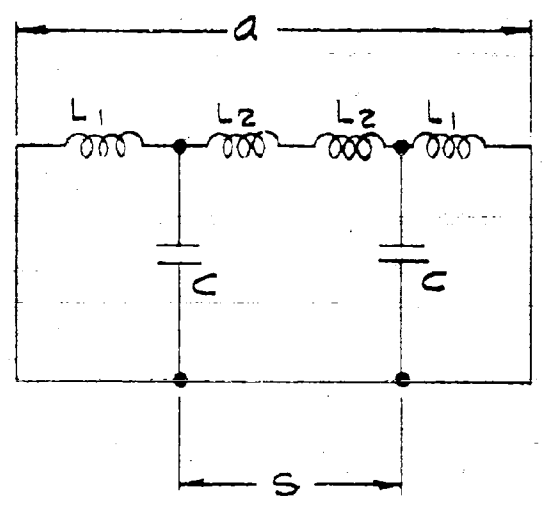
- $a = 0.471 \pm .002$
- $b = 0.219 \pm .002$
- $d = 0.093 \pm .0005$
- $s = 0.118 \pm .001$
- $r_1 = 0.015 \text{ MAX.}$
- $r_2 = 0.019 \pm .002$

11.0 - 26.5 Gc RIDGE
WAVEGUIDE CONFIGURATION
FIG. 1



EQUIVALENT CIRCUIT
SQUARE RIDGE
CORNERS

a



EQUIVALENT CIRCUIT
ROUNDED RIDGE
CORNERS

b

FIG. 2

FACTUAL DATA

I. INTRODUCTION

This contract consists of the design and development of components for measurement and systems application in the 11.0 - 26.5 Gc frequency range. The components were built in the double ridge waveguide configuration as shown in Figure 1. Electrical characteristics and mechanical construction of the waveguide will be described briefly followed by a description and discussion of each component.

Electrical Characteristics

The effect of inserting ridges into rectangular waveguide is to produce a capacitance (C) at the ridge step (see Figure 2a). This capacitance will lower the cutoff frequency of the TE_{10} mode. The capacitance occurs in a low electric field region for the TE_{20} mode and therefore the loading effect is less in this case. The overall effect is to increase the frequency range for propagation of the TE_{10} mode without second and higher order modes appearing. Rounding the ridge corners will increase the power handling capabilities of the ridge waveguide by reducing the electric field strength at the sharp corners, since electric field intensity always increases in the vicinity of sharp corners. The electric field intensity at the ridge corner is reduced with increased rounding as indicated in Figure 3. The rounding will introduce inductances into the equivalent circuit, resulting in the more complex T-junction circuit indicated in Figure 2b. This equivalent circuit is used to calculate the characteristic impedance and cutoff frequency of the rounded guide. Optimum dimensions for a series of double ridge waveguides with a 2.4:1 bandwidth were determined by the NARDA Microwave Corp.

ELECTRIC FIELD STRENGTH OF ROUNDED CORNERS

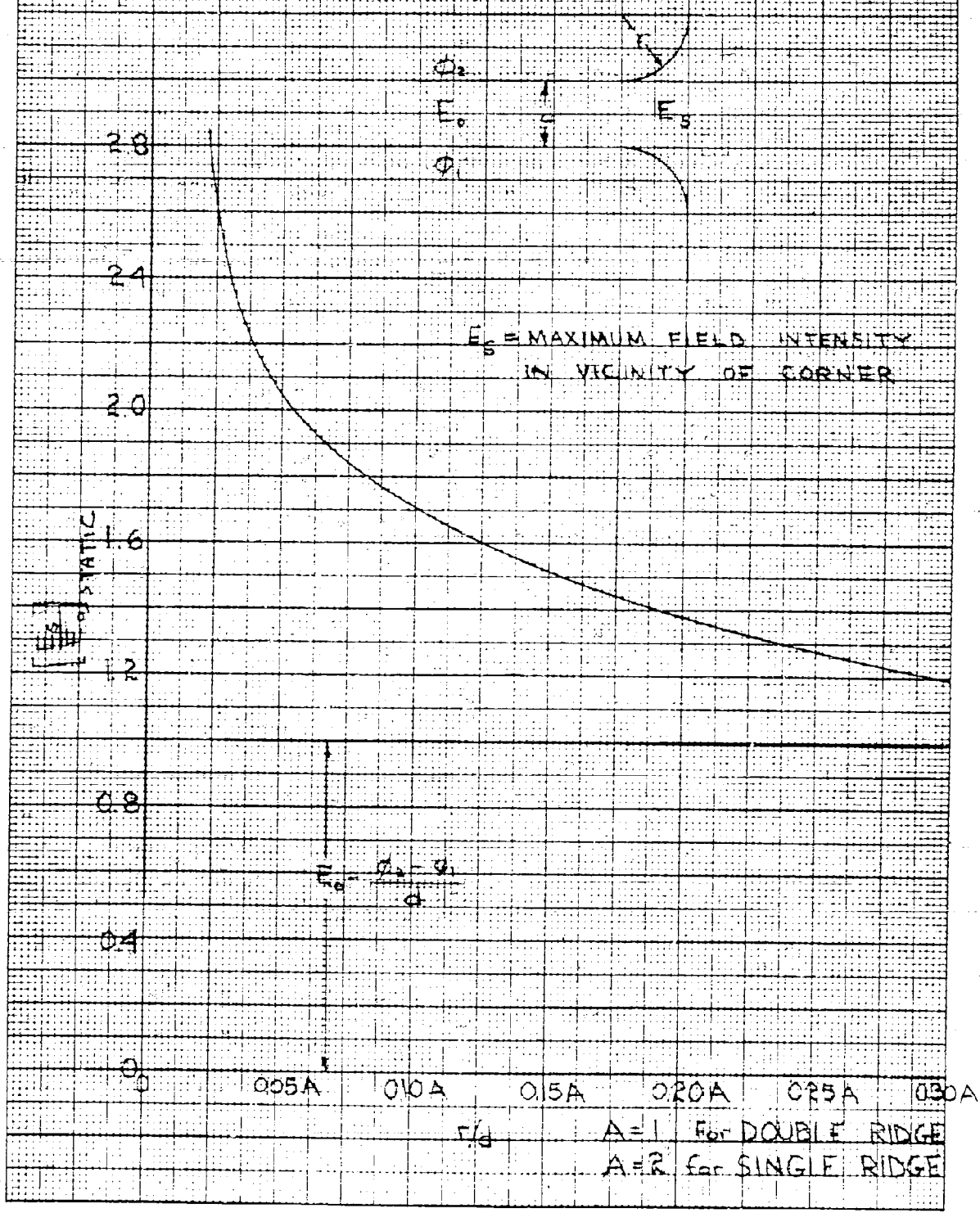


FIG 3

under Contract No. DA 36-039 SC 78187¹ (See Figure 4). Components were developed under that contract in the 4.75 to 11.0 Gc range. The present contract involves extending this development to the 11.0 to 26.5 Gc range. Dimensions for ridge waveguide in this frequency range, as well as others which were determined under DA 36-039 SC 78187, are under consideration for industry standardization by the Electronic Industries Association.² A detailed theoretical analysis of ridge waveguide may be found in References 1, 3, 6, 8 and 9.

Power Handling and Attenuation

The power handling and attenuation characteristics of the 11.0 to 26.5 Gc double rounded ridge waveguide compared to rectangular guides covering this frequency range are given in Figures 5 and 6. The ridges reduce the power handling to 1/4 that of RG-53/U, which has about the same a and b dimensions. The attenuation is of the same magnitude as in RG-53/U waveguide, but is considerably greater than RG-91/U and RG-52/U waveguides. The characteristics of ridged waveguide are ideal for use in low power broadband applications. Considerable savings in size and weight may be achieved when the ridge guide is used at the lower end of the frequency range, compared to rectangular guide for the same frequencies. For example, the ridged guide cross section in the 11.0 to 26.5 Gc range is 1/4 that of X-band guide for 11.0 to 12.4 Gc. The higher attenuation of the ridged guide may be disadvantageous in some applications, however, where only short runs of waveguide are involved the absolute difference will be small.

¹See Reference 1

²See Reference 2

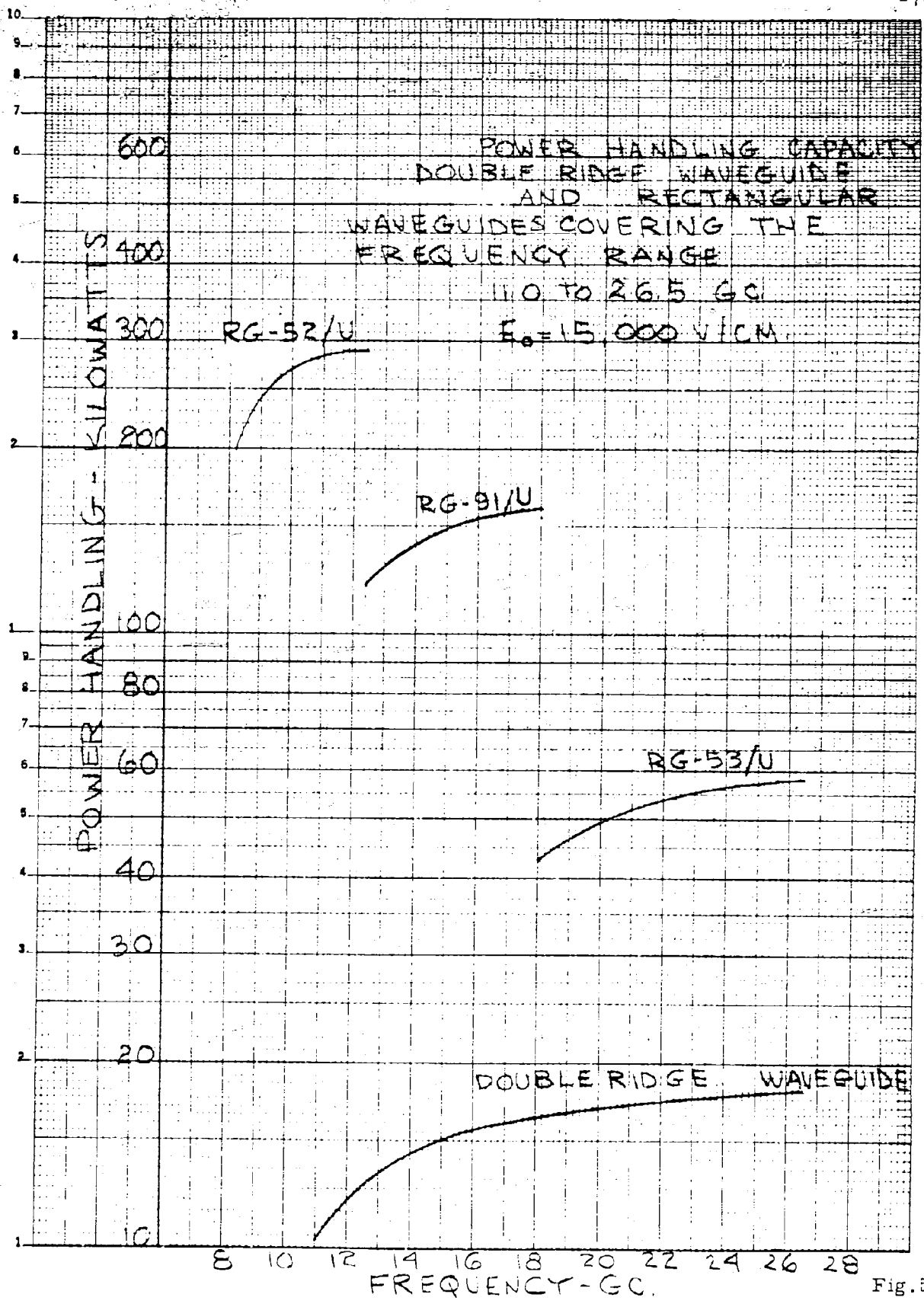
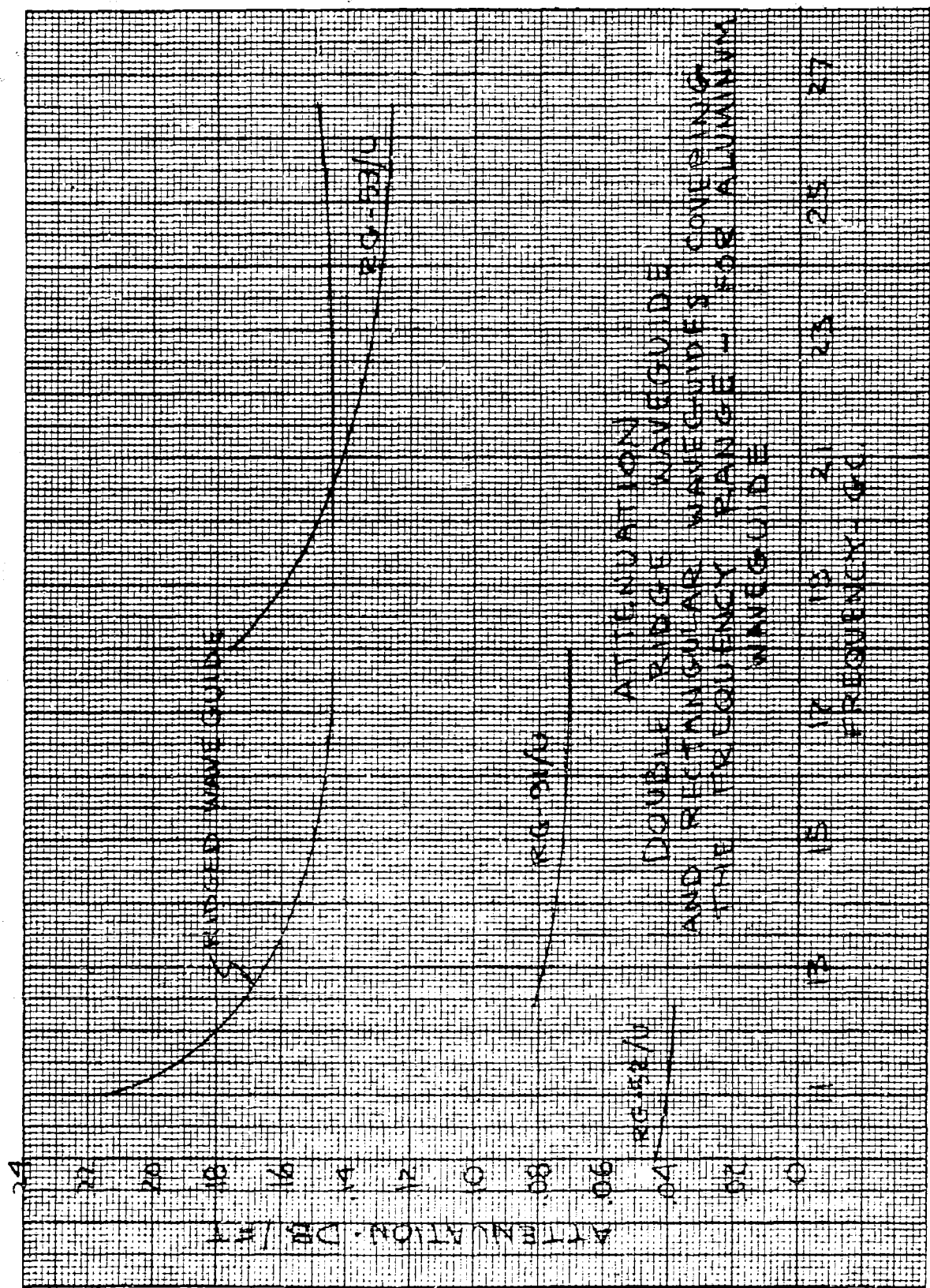


Fig. 5



ATTENUATION ATTENUATION
 DOUBLE RIDGE WAVEGUIDE
 AND RECTANGULAR WAVEGUIDES COVERING
 THE FREQUENCY RANGE - FOR ALUMINUM
 WAVEGUIDE

11 12 13 14 15 16 17 18 19 20 21 22 23 24 25 26 27
 FREQUENCY - GHz

Fig.6

Fabrication of Ridge Waveguide.

A critical factor in the fabrication of waveguide in small sizes is that of holding tolerances. This problem caused considerable difficulty during the contract. It was originally decided to sub-contract the manufacture of extruded waveguide in the necessary size. This would greatly simplify the construction of many of the components, compared to machining the waveguide out of solid bar stock. After many attempts and considerable experimentation by the firm (Standard Metals, Inc.) who undertook the extrusion job it was decided that the waveguide could not be extruded to the required tolerance. Most components produced under this contract were finally machined from solid stock. The closest tolerances that can be held by present extrusion methods and the resulting maximum percentage deviation of characteristic impedances is compared to the required tolerances and corresponding impedance variations in the following table.

<u>DIMENSION</u>	<u>REQUIRED</u>		<u>EXTRUDED</u>	
	<u>Tolerance</u>	<u>%Imp. Var.</u>	<u>Tolerance</u>	<u>% Imp. Var.</u>
a	±.002	0.74	±.002	0.74
b	±.002	0.84	±.002	0.84
d	±.0005	1.50	±.002	6.00
s	±.0005	0.30	±.002	1.20
TOTALS		3.38		8.78

The required tolerance will give maximum mismatch between two mating guides of 1.07 VSWR. The extruded tolerances would give 1.18 VSWR. It was determined that a 1.08 VSWR which would result in less than 0.2% of the power reflected, should be the maximum allowable VSWR for component use in ridge guide. In most of the

components, precision machining produced tighter dimensional tolerances than were required, so that precise measurements may be taken on future components. In two cases (rotary joint and attenuator) a different fabrication method was used. The ridges were screwed or soldered into rectangular guide having the same "a" and "b" dimensions as the ridge guide. This method is to be avoided for ridge guide components in general since it requires custom machining of the ridges to obtain the required gap dimension between the ridges. It is also difficult to insure good contact between ridge and guide. Electroforming of the guide was investigated, but found to be expensive and only applicable for short lengths of guide. It was found that for the present, the most economical method for making ridge guide to tolerance in this small size is by machining. Detailed machining and assembly procedures for the components may be determined from a perusal of the component detail drawings.

II. DESCRIPTION OF COMPONENTS

The following components were designed and fabricated for this contract:

1. Precision Slotted Section
2. Adapter, double ridge to RG-52/U rectangular guide
3. Adapter, double ridge to RG-91/U rectangular guide
4. Adapter, double ridge to RG-53/U rectangular guide
5. Sliding Termination
6. Tunable Crystal-Bolometer Mount
7. Variable Attenuator
8. E-H Tuner
9. Tunable Waveguide Short
10. Rotary Joint
11. Directional Coupler
12. Balanced Mixer
13. Flanges

The design of each component will be discussed and final data presented in the following sections. Photographs of typical components are given in Figures 7 to 10.

Precision Slotted Section

The slotted section is one of the most important test components since it is used as a standard of impedance to measure other components. The residual VSWR of the slotted section must be low in order to measure the VSWR of other components accurately. A method of sampling the field in the transmission line must be provided such that the distortion due to sampling introduces negligible error.

The slotted section which was made for this contract consists of a double ridge waveguide main line containing a slot, a probe section

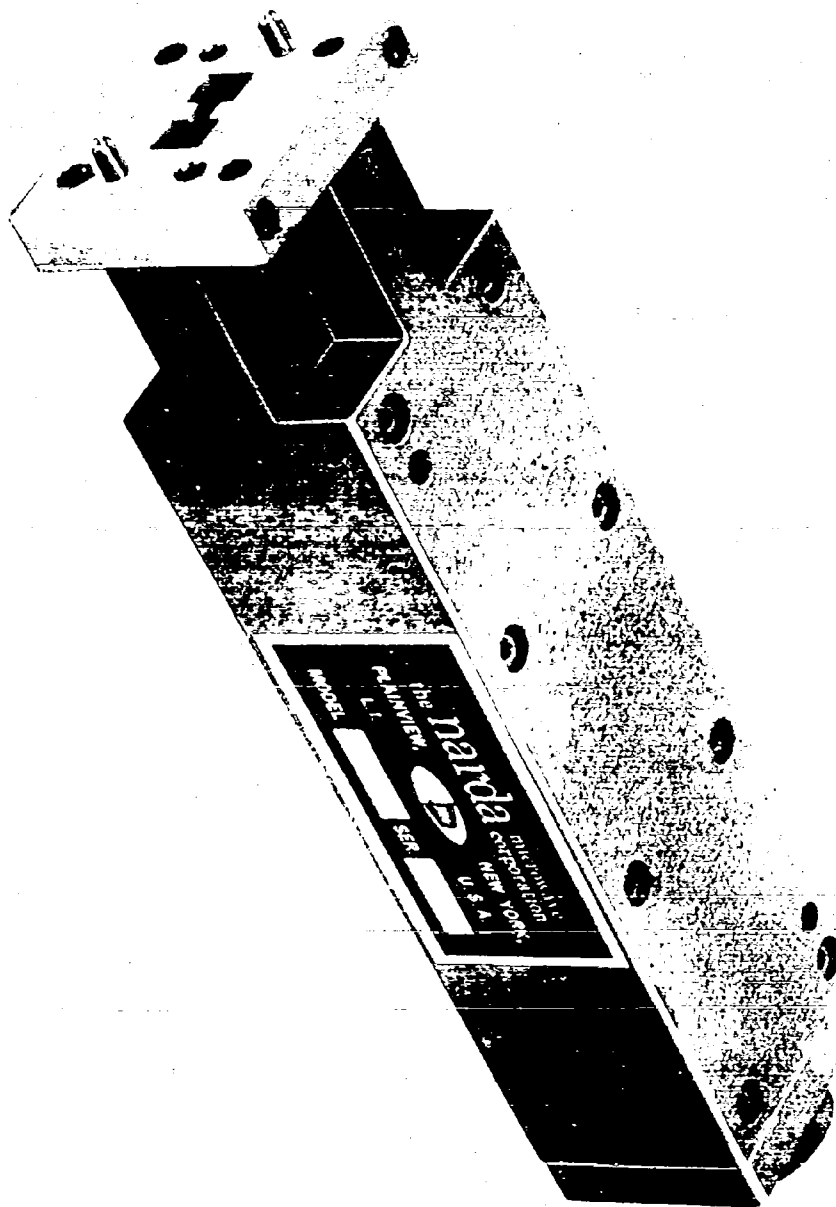


Fig. 7

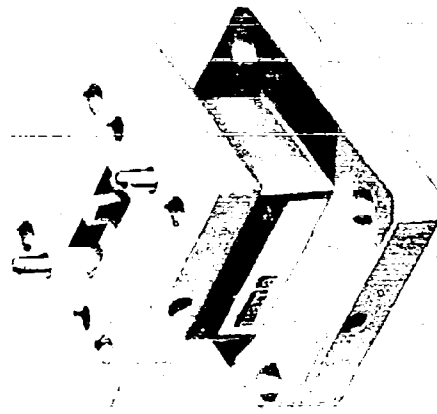
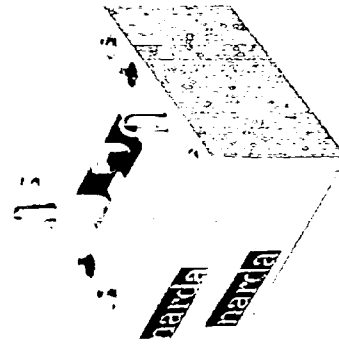


Fig. 8

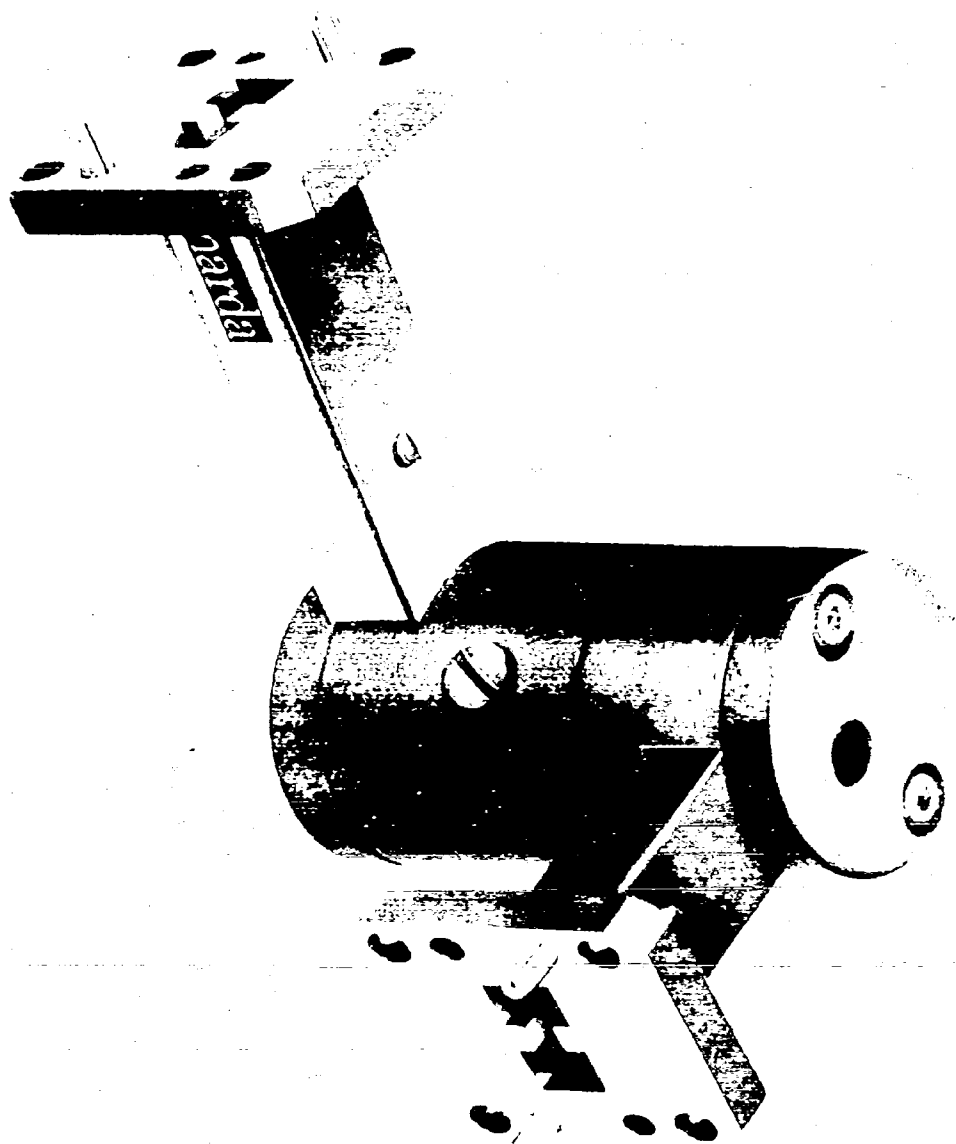


Fig. 9

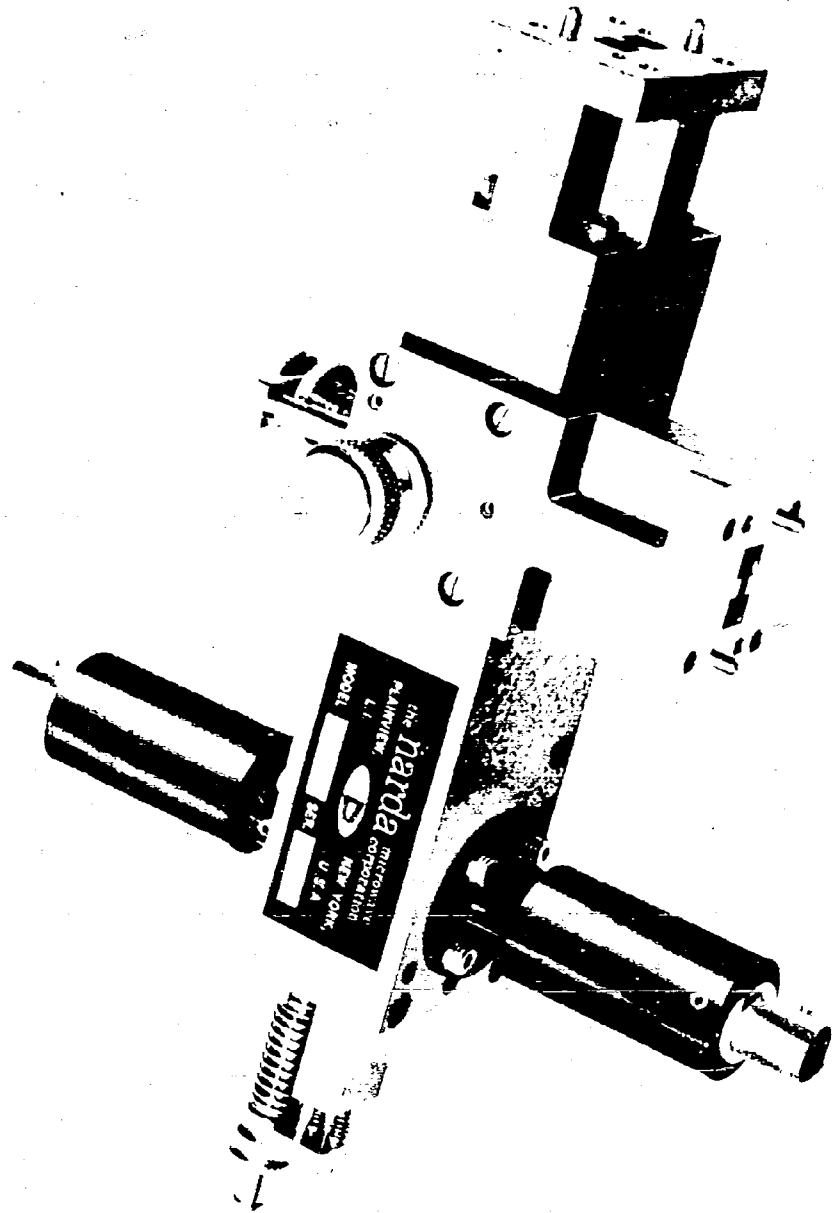


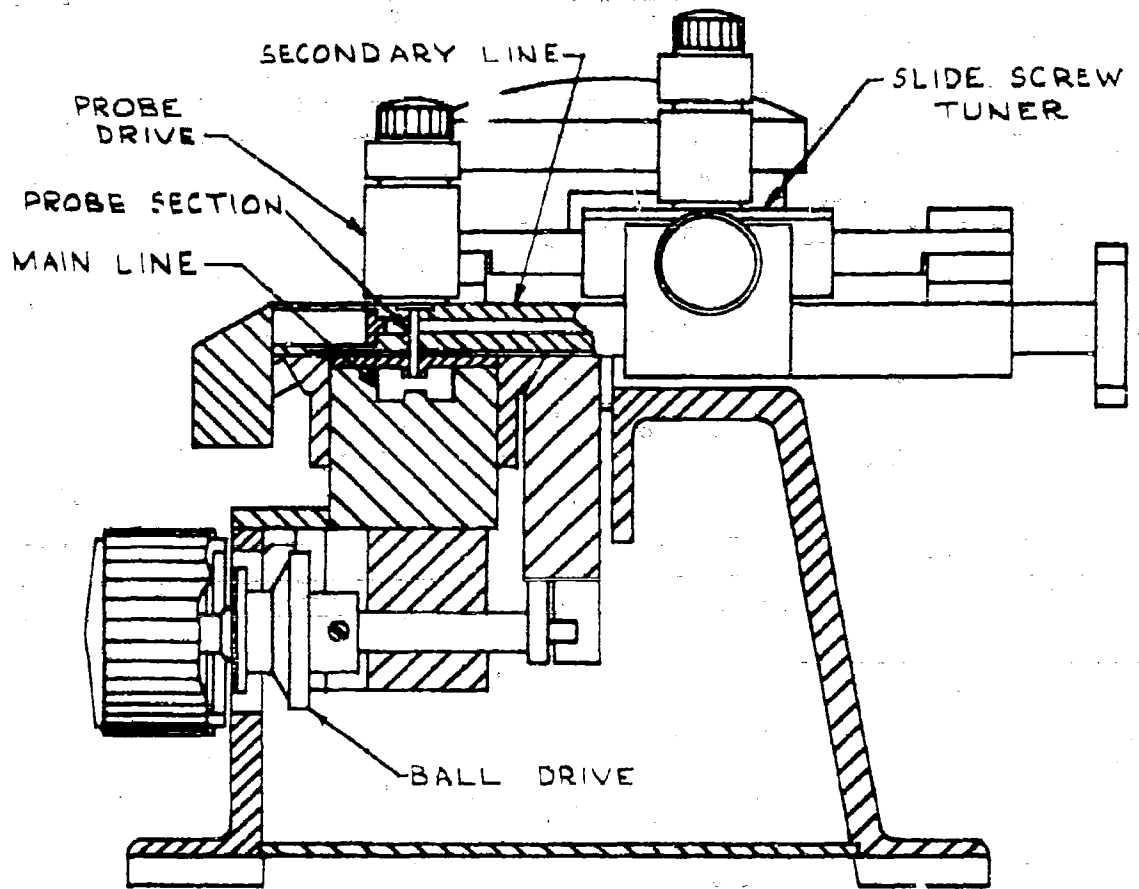
Fig. 10

and a secondary double ridge waveguide section containing a slide screw tuner (see Figure 11). A detector mount containing a bolometer or a crystal is connected to the secondary line and is in turn connected to a VSWR amplifier for measurements. The probe, a 0.006 inch diameter teflon coated wire, is extended into the main line by means of a screw driven mechanism. The energy coupled to the probe is conducted through a coaxial section into the secondary guide. The slide screw tuner is used to match the detector mount to the probe transition section of the secondary guide.

The detector for the slotted line may be either one of the double ridge tunable crystal-bolometer mounts provided in the contract, or it may be a rectangular waveguide detector used with the appropriate adapter to double ridge guide.

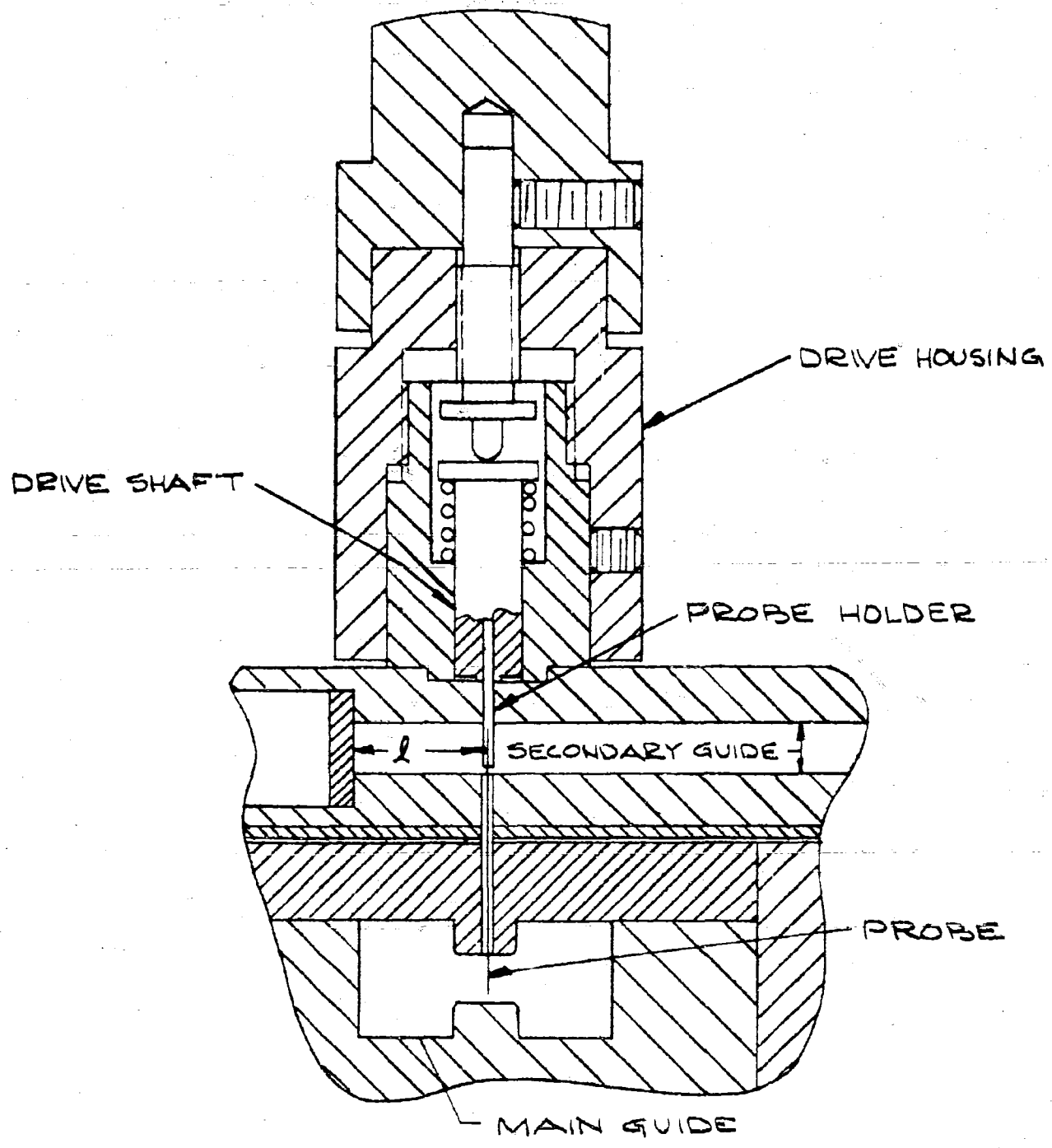
The slotted section has a precision milled tellurium copper main transmission line. Tellurium copper is used because of its machinability and its ability to retain high conductivity under corrosive conditions. The narrowest slot width practical mechanically was used to keep the residual VSWR low. Tapers $(3/4)\lambda_g$ long at the lowest frequency are used at the ends of the slot to reduce the residual VSWR due to slot reflections. Accurate centering of the slot to within 0.0005 inches was accomplished by precision machining and assembly methods in order to prevent the appearance of slot waves. Probe travel is greater than $(1/2)\lambda_g$ at the lowest frequency in the band.

A precision calibrated dial indicator is provided to accurately measure relative probe travel. This is desirable for precise impedance measurements. The least count on the indicator is 0.0005 inches, which



SLOTTED SECTION

Fig. 11



SLOTTED SECTION PROBE DETAIL

Fig. 12

is $0.001 \lambda_g$ at the highest frequency. Phase can therefore be measured to a least accuracy of 0.36 degrees or 22 minutes. Smooth carriage travel without backlash is obtained by using a planetary ball reduction drive coupled to a rack and pinion. Possible slot leakage and resonances are suppressed by using a disk of absorbent NARDA IRON material around the probe section.

Empirical methods were used to determine the dimensions of the secondary line probe transition section. The back cavity dimension " l ", see figure 12, was set to give the flattest coupling response over the band. Resonances which were found in the secondary line coupling response were eliminated by changing the probe-holder length. The amount of probe insertion into the guide was limited to avoid distortion or 'pulling' of the main line power. Final test results are given in Figure 13. The residual VSWR is 1.04 maximum and averages 1.02 over a good part of the band. Slope is well under 1.01. Coupling to the secondary line is a minimum of 19.0 db down from the main line for negligible "pulling" effect.

Adapters, Double Ridge to Rectangular

Adapters were fabricated for the three rectangular waveguides that cover the 11.0-26.5 Gc band. These include adapters to RG-52/U (11.0-12.4 Gc portion of the band); RG-91/U (12.4-18 Gc band); and RG-53/U (18.0 -26.5 Gc Band). The transition from ridge to rectangular guide is made by means of four ridge steps (see Figure 10). The impedance required for each step is determined from Tehebscheff

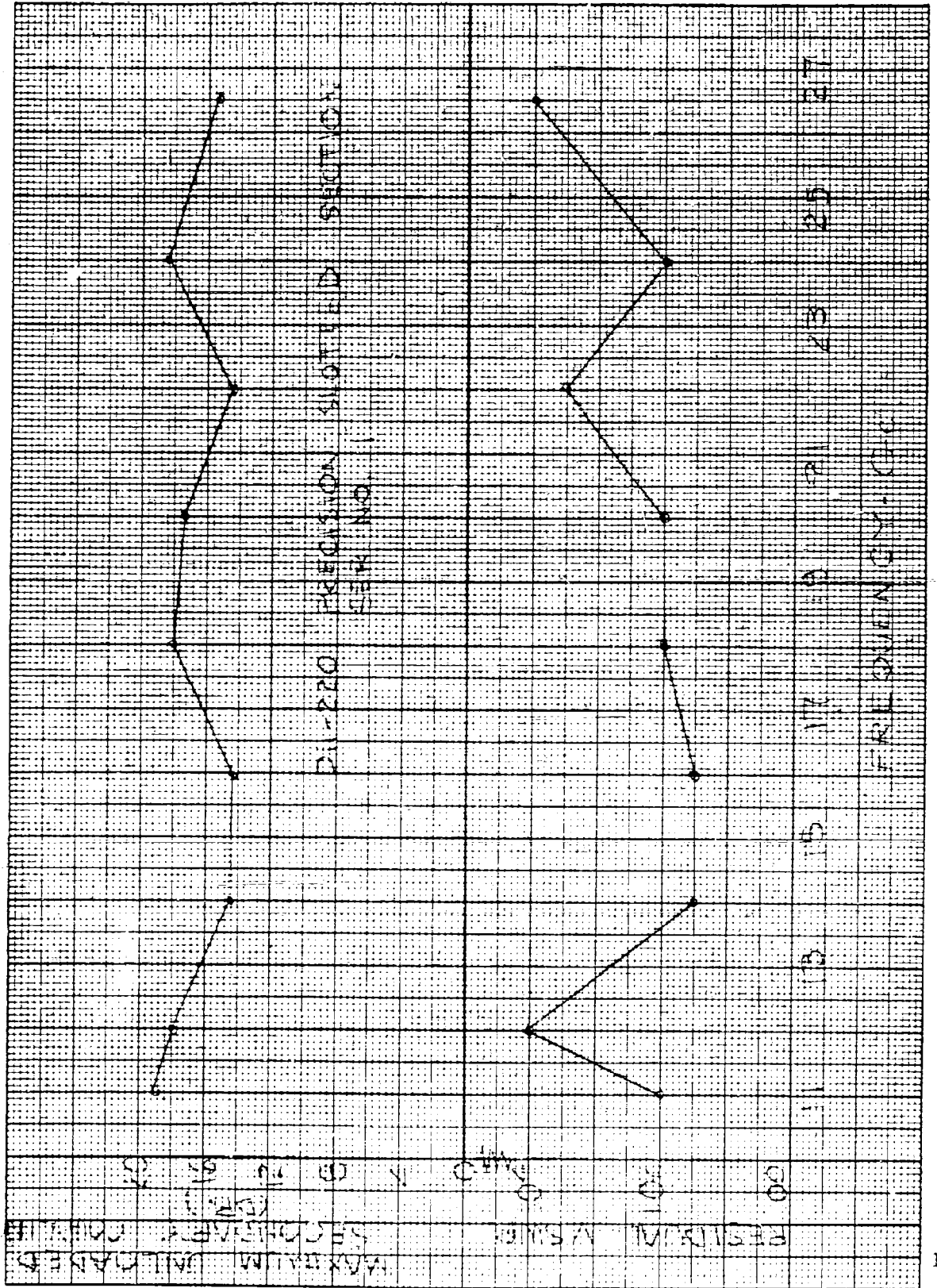
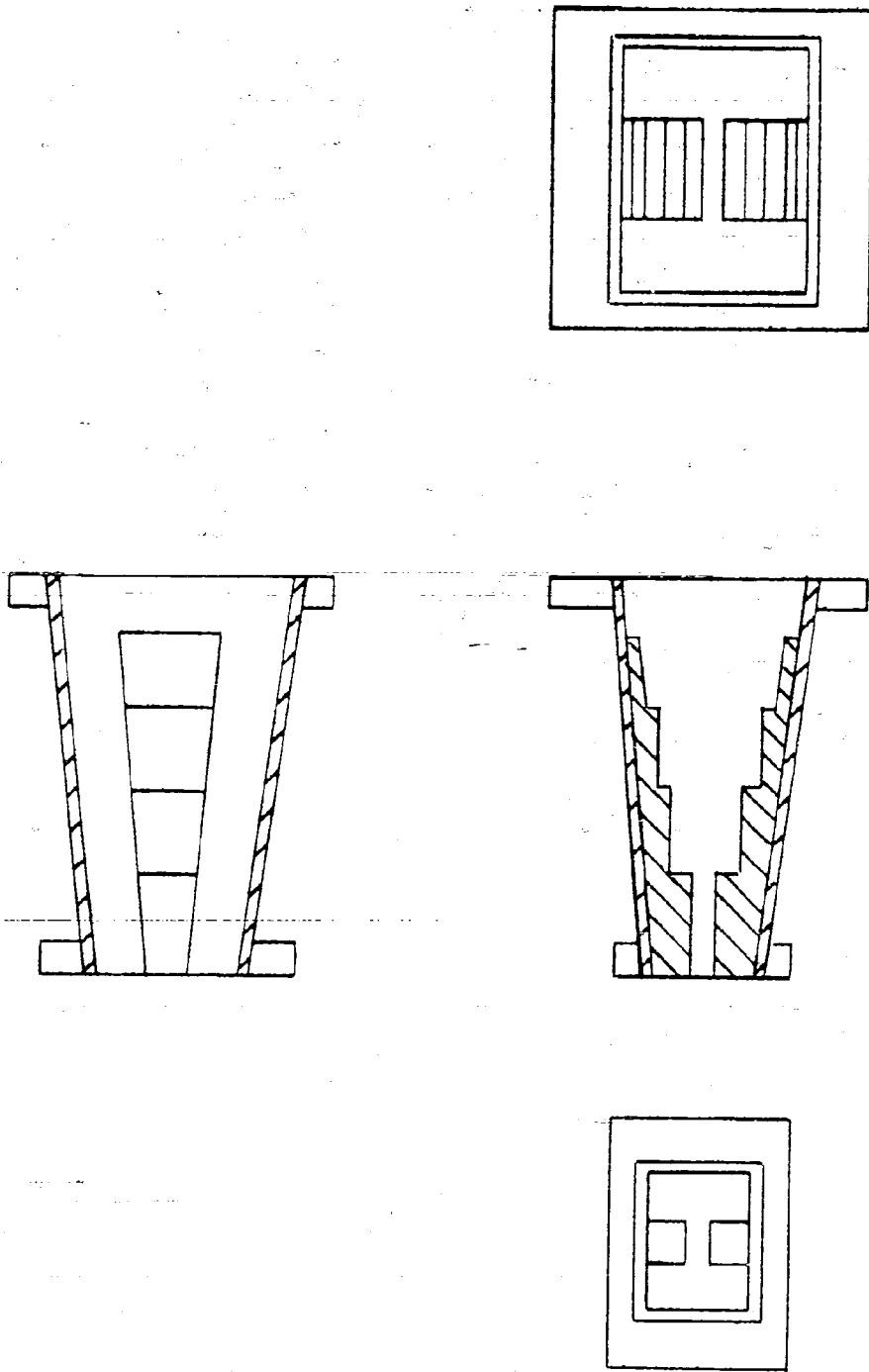


Fig. 13



DOUBLE RIDGE TO RECTANGULAR WAVEGUIDE
ADAPTER

FIGURE 14

coefficients calculated as a function of the rectangular guide bandwidth. The ridge configuration for each step section is determined by solutions of the transmission line equation to obtain the appropriate impedance across the step. Ridge corners are made square to simplify calculations and to avoid extremely difficult matching problems. The "a" and "b" dimensions are tapered linearly from the ridge to rectangular guide. The "s" dimension is also tapered to maintain a constant s/a ratio in order to simplify calculations. The only parameter that must be determined is the "d" dimension. The step length is nominally made equal to $\lambda_g/4$ as determined at the center of the step. This length is reduced by approximately 4% in order to compensate for the discontinuity capacitance at the step-junction. The step capacitance effectively increases the electrical length of the step, so the physical length must be shortened appropriately. Impedances for the sections are determined from available graphs. See Appendix A for a sample calculation. Four steps were chosen as the minimum number which would give the specified characteristics. Accuracy was assured by holding close tolerances on the steps and calculating step impedances to within 1/2% from the Tchebyscheff value required across the step. In the original design, the variation in the b/a ratio from the ridge to rectangular guide was neglected in the calculations. This was done to simplify calculations since it appeared that the differences would be negligible. Initial tests of the RG-91/U and RG-53/U transitions showed a higher VSWR than was anticipated. A detailed evaluation indicated that the higher VSWR was due to erroneous impedance calculations that

resulted from neglecting the b/a ratio change. Recalculating the step design and making the appropriate modification on the transitions resulted in units which were all within the specified VSWR of 1.08. See Figure 15 for final data on the three transitions.

Sliding Termination

A sliding matched termination has been made in double ridge guide as shown in Figure 16. L584 grade synthane strips are used as lossy elements in the unridged portion of the guide. Two vanes, 2-29/32 inch long by 0.020 inch thick, are angled from the narrow wall to the ridged. Good contact at the wall and ridges is assured by leaf spring mounting. Minimum travel is greater than 1 inch to provide greater than $(1/2)\lambda_g$ travel at the lowest frequency. The VSWR of the termination is within the specified value of 1.02 (see Figure 17).

Tunable Crystal Bolometer Mount

A tunable detector mount was designed (sketch shown in Figure 18) which incorporates a slide screw tuning mechanism. It is useable with a coaxial (1N26) cartridge detector; either crystal or bolometer.

It was necessary to use a coaxial transmission line mount for the detector because of the dimensions of the 1N26 cartridge (shown in Figure 19). This necessitated a waveguide to coaxial transition which was built into the unit.

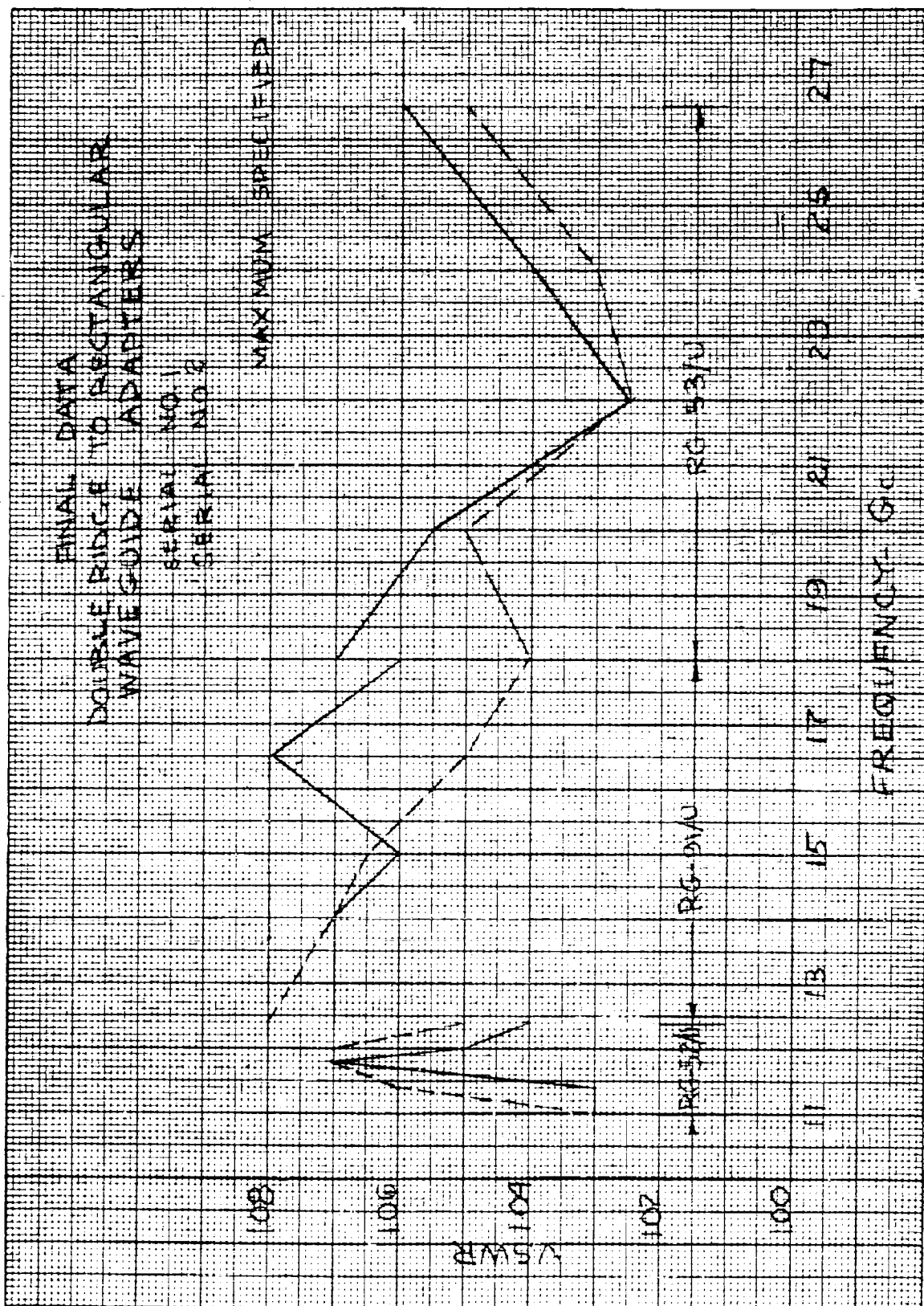
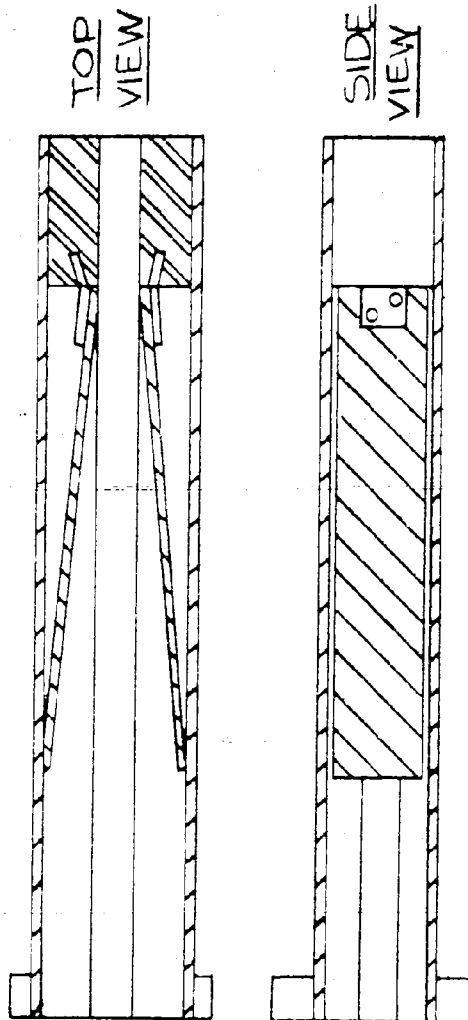


Fig. 15



SLIDING MATCHED TERMINATION

Fig. 16

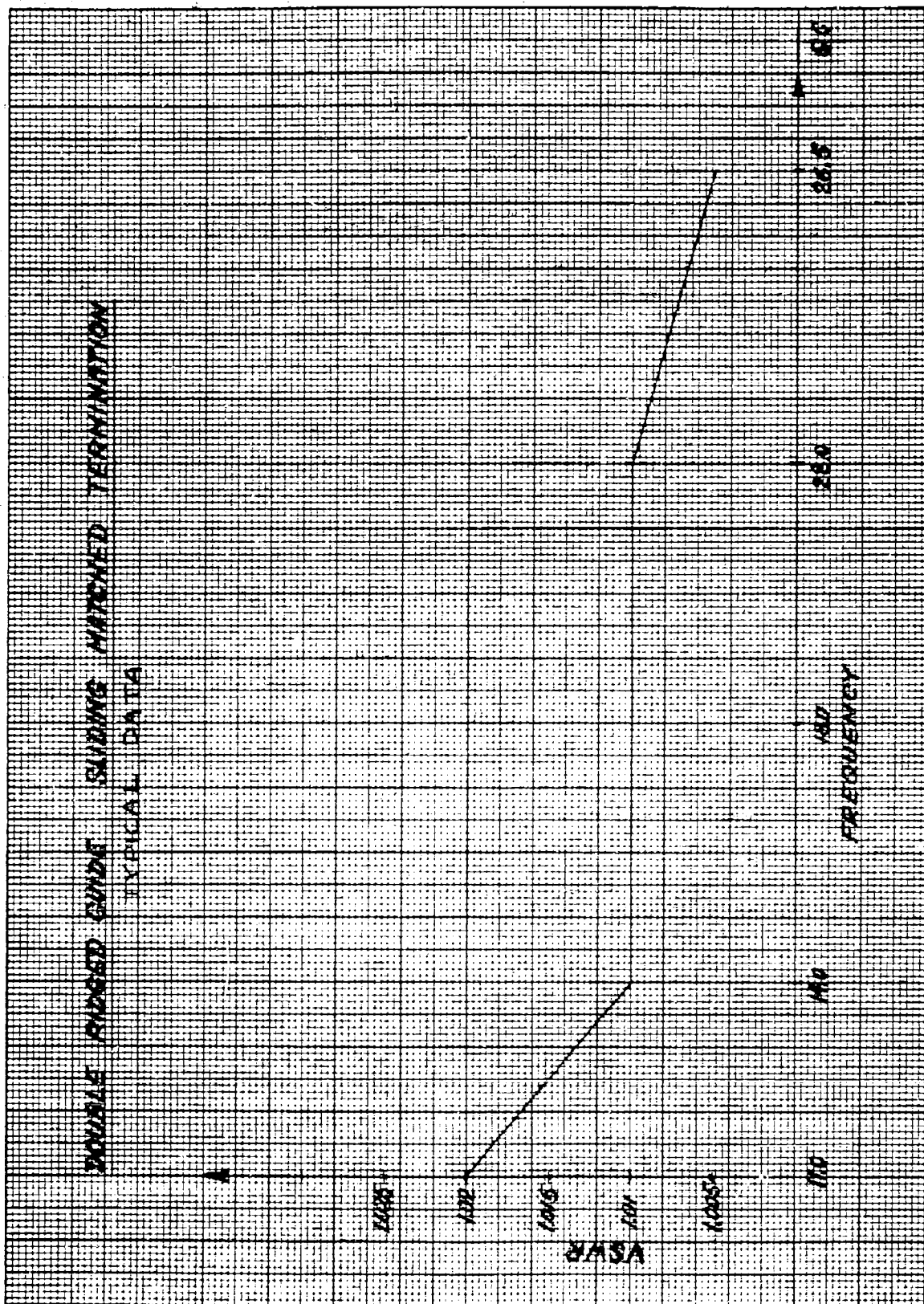
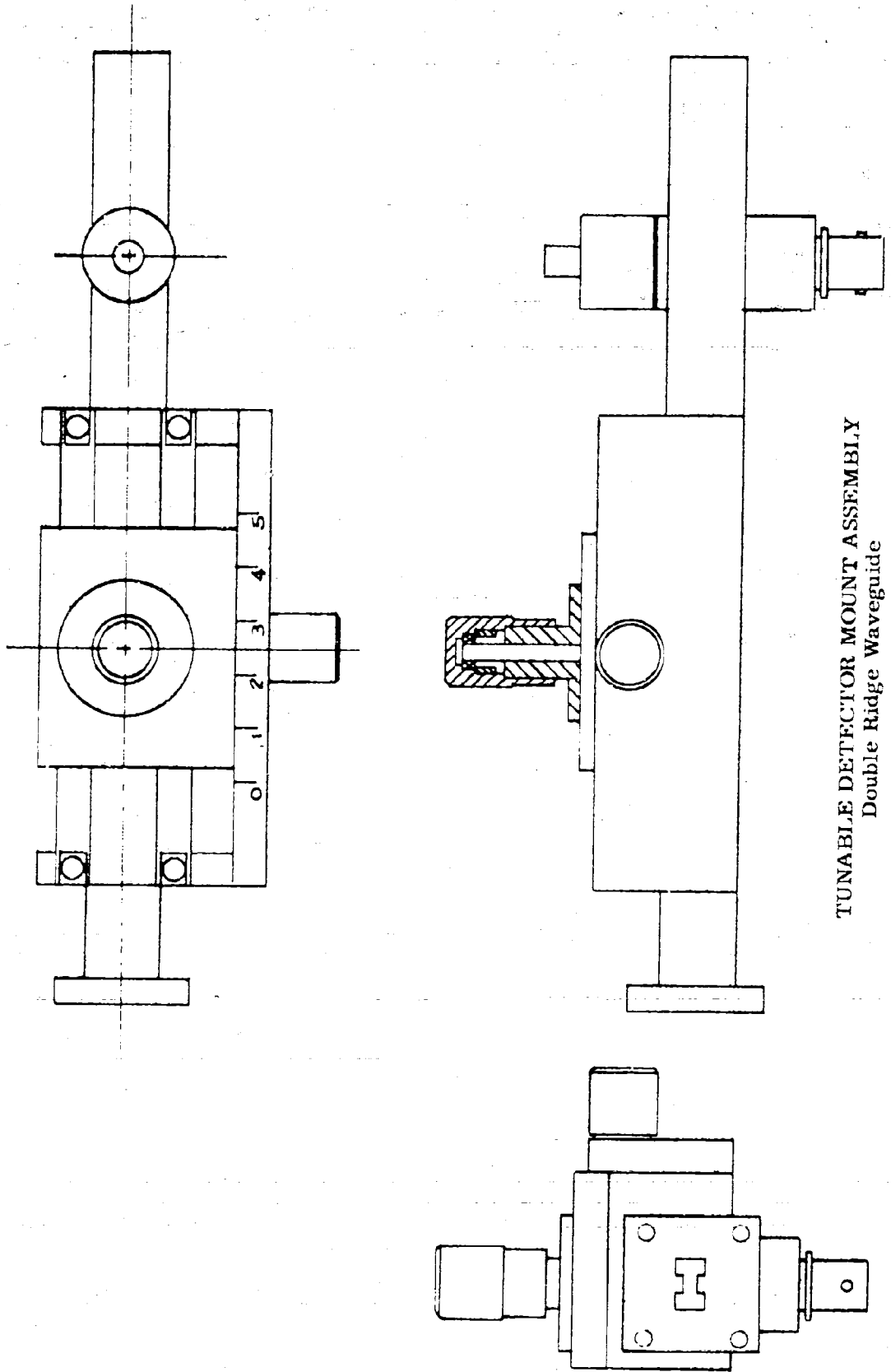
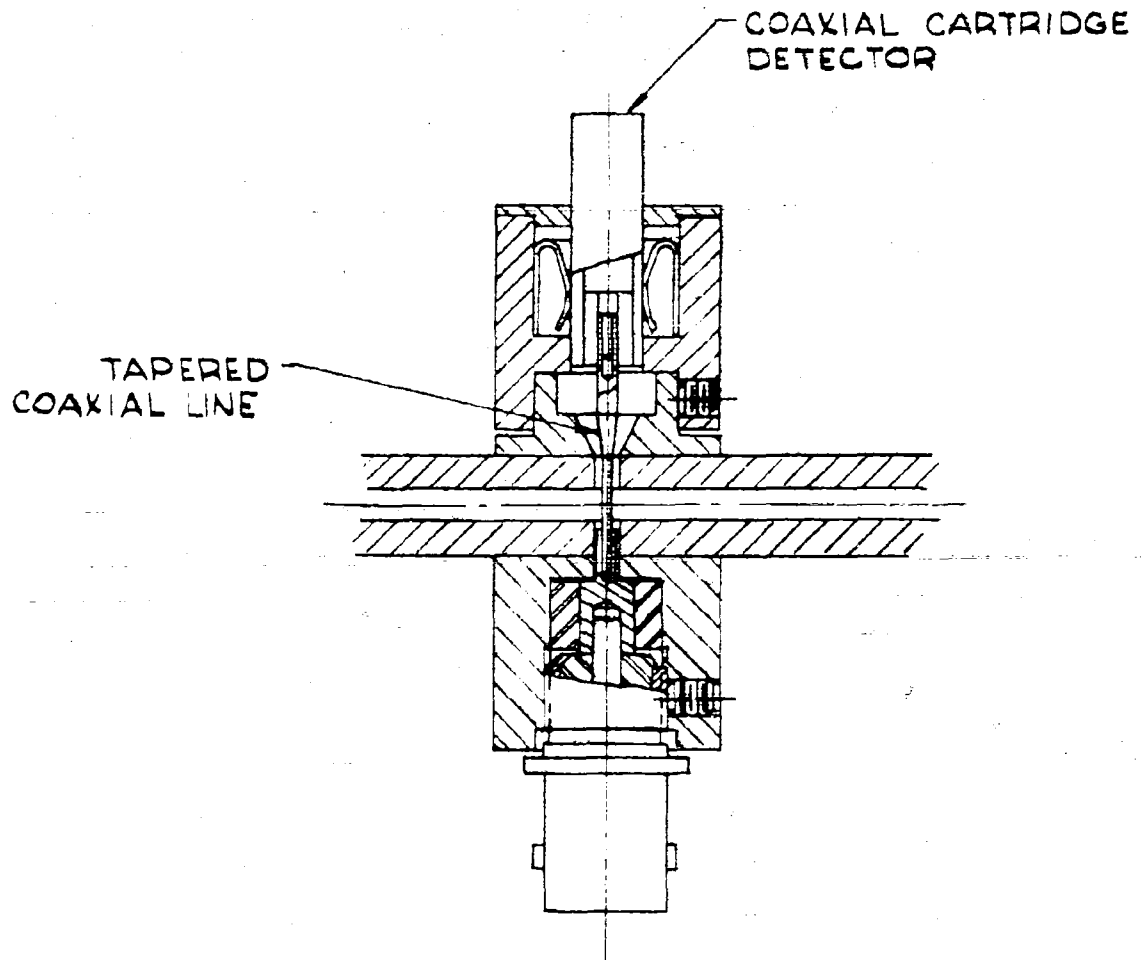


Fig. 17



TUNABLE DETECTOR MOUNT ASSEMBLY
Double Ridge Waveguide

Fig. 18



Detail of Bolometer Mount Showing Detector Cartridge
and Waveguide to Coaxial Adapter

Fig. 19

Sometimes when a coaxial cartridge of this type is used, the outer conductor of the cartridge is cut back to expose the center conductor (Figure 20a), which is then used as a probe into the main line of the mount. This technique was not feasible in the case of the ridge waveguide mount because the ridge was too narrow for this type of construction. The probe would be required to extend through the ridge as the center conductor of a coaxial line. The minimum inside diameter of the outer conductor for 50Ω characteristic impedance would be .145 inch while the ridge is only 0.118 inch wide (Figure 20b). The design of the waveguide to coaxial transition shown in Figure 19 utilizes a smaller diameter center conductor which tapers to the sufficiently larger size to form a finger connector to the pin of the detector. The use of the smaller diameter center conductor allows the 50Ω characteristic impedance to be presented throughout the transition.

The use of a coaxial cartridge detector obviates the possibility of using the mount across the band with no tuning adjustment. Also, since impedance of a crystal varies greatly, with frequency, this constitutes another demand for the addition of a matching device. These effects are indicated in the "untuned" curve of Figure 21. The back cavity dimension was chosen to give best match at mid-band (18.0 Gc). The cartridge VSWR measurements indicated two symmetrically placed VSWR spikes across the frequency spectrum. The third VSWR spike at the low end of the band is probably due to the geometry of the mount.

The effect of the slide screw tuner is shown by the "tuned" curve

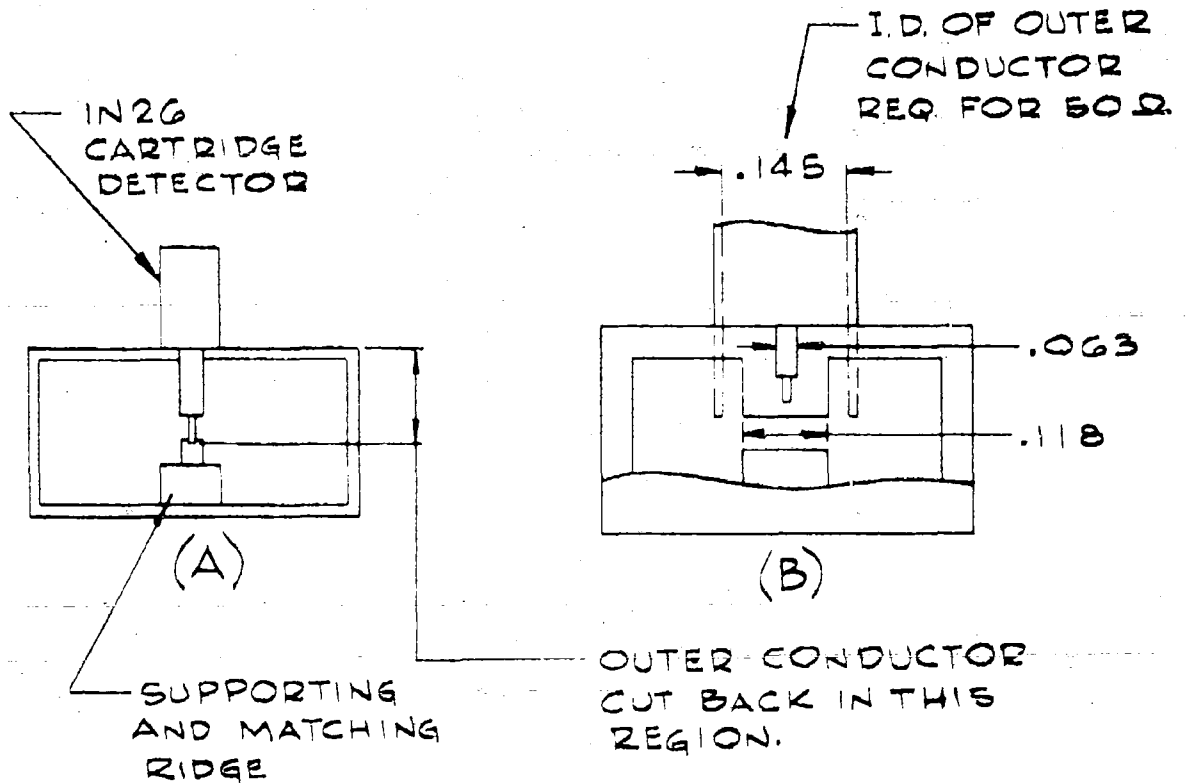


Figure 20: Mounting of Coaxial Cartridge Detector in Waveguide

- a). Sketch showing cut-back case approach (cross section of waveguide)
- b). Cross section of double ridge guide showing interference between ridge width and required coaxial conductor dimensions for 50Ω line.

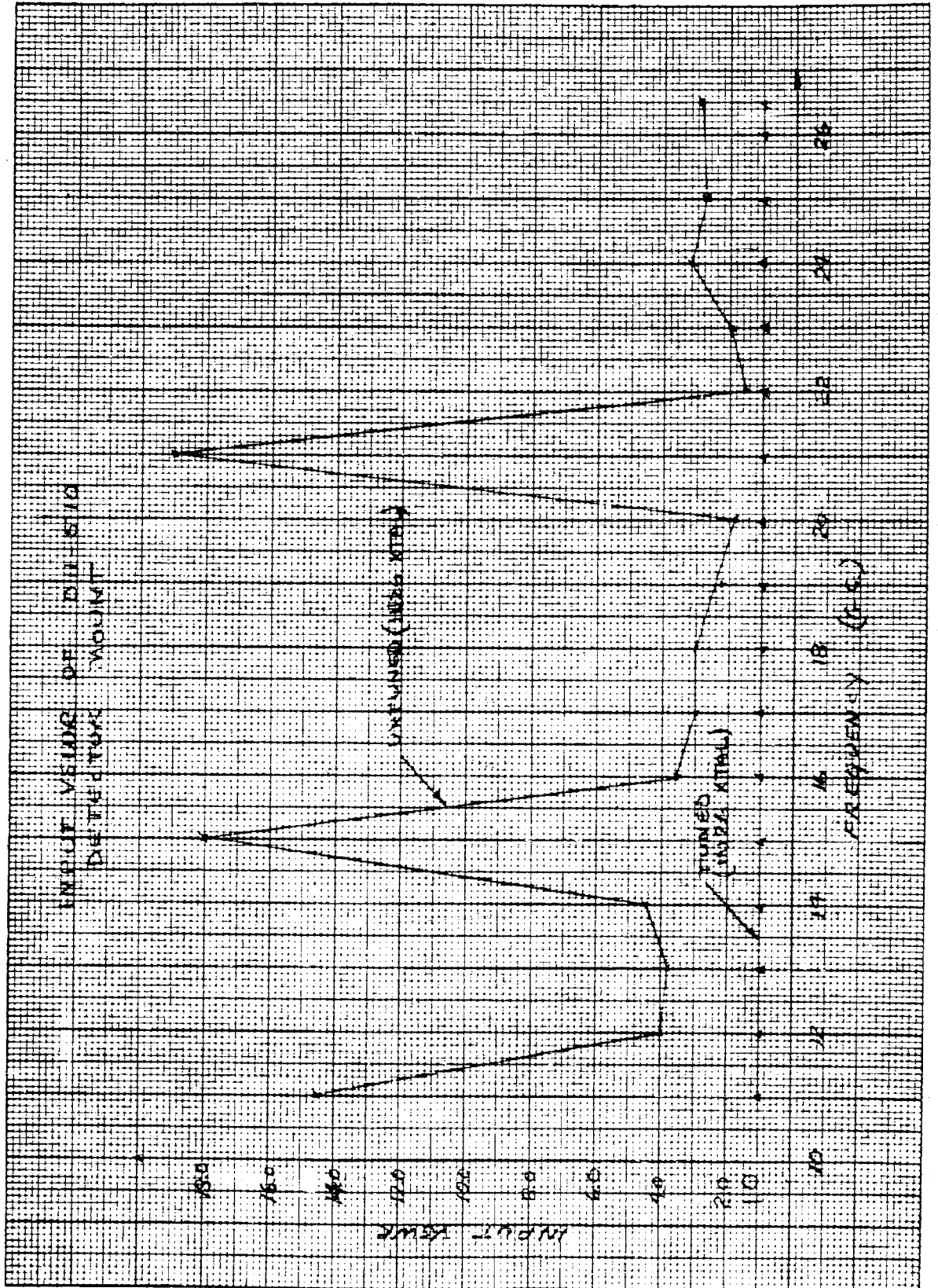


Fig. 21

which indicates that a match of 1.06 or better was obtained across the band with a 1N26 crystal. A bolometer (in a 1N26 case) should give equal or better results since the bolometer impedance is constant while that of the crystal varies widely.

Variable Attenuator

A variable flap attenuator was designed for the 11.0 to 26.5 Gc frequency range. The basic mechanical configuration of the attenuator is shown in Figure 23.

The input (Section A-A) is a double ridge configuration with sharp corners (Figure 24b) having the same TE_{10} cutoff wavelength as the standard rounded corner guide (Figure 24a).

The infinite frequency impedance of the rounded ridge guide and square ridge equivalent are both 188Ω . Since the λ_{c10} is the same, the impedance of both guides will be identical at any frequency. The only mismatch involved will be the step between the ridge heights shown in Figure 22.

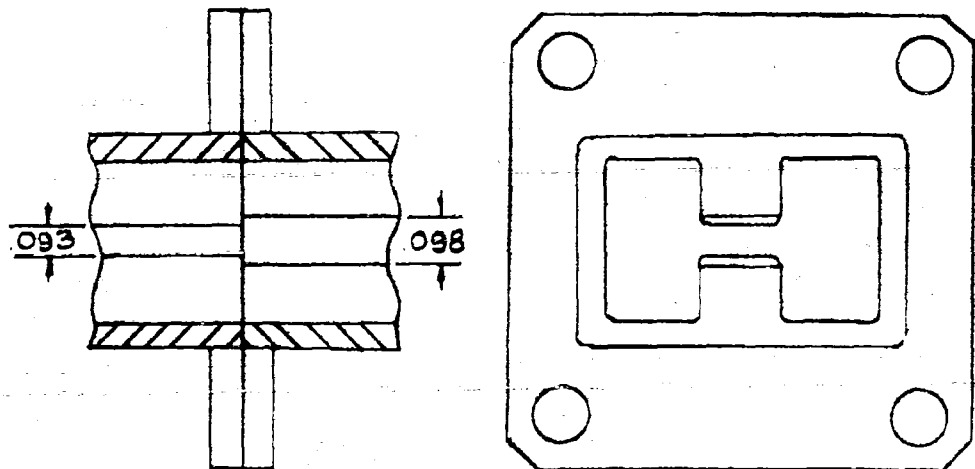
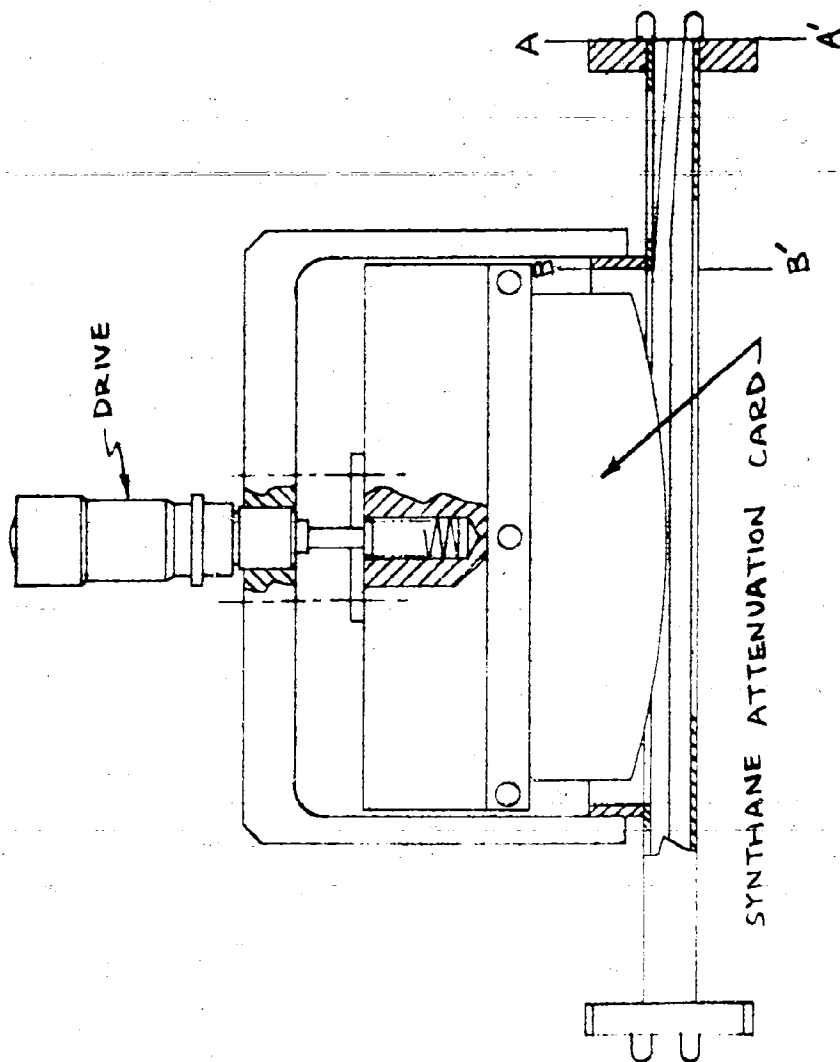
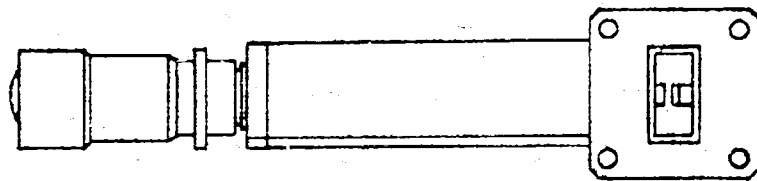
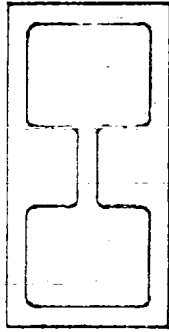


Fig. 22



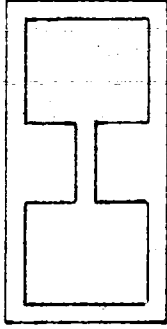
DOUBLE RIDGE GUIDE ATTENUATOR

Fig. 23



Standard Double Ridge
Configuration

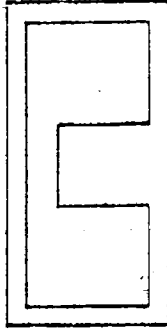
(a)



Double Square Ridge Corner
Configuration

(Section A-A' of Figure 19)

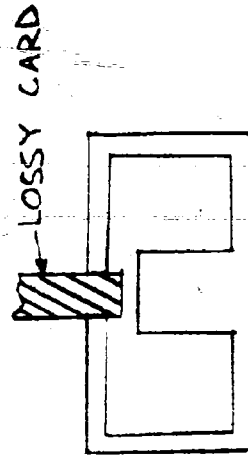
(b)



Single Square Ridge Corner
Configuration

(Section B-B' of Figure 19)

(c)



Attenuation Card Section

(d)

VARIABLE ATTENUATOR CONFIGURATIONS

Fig. 24

The step capacitance may be found using the graph of Figure 25. The mismatch may be calculated to be less than 1.01.

The upper ridge is then tapered down to the waveguide wall and the lower ridge tapered up to give the single ridge waveguide configuration shown in Figure 24c. This section was designed to have the same first mode cutoff and the same impedance as Section A-A'. The second mode cutoff was found to be 24.0 Gc which is within the band. However, no deterioration in the VSWR or attenuation characteristics was found at 24.0 Gc or above. This would indicate either that the secondary mode was not being excited or that if excited the power carried was substantially below the primary mode power.

The attenuator card is inserted through a slot in the unridged waveguide wall in the center section (Figure 24d). It was found that if the slot is made narrow enough (0.050 or less), tapers at the slot ends are not necessary. The residual VSWR from this slot was found to be less than 1.05. The attenuator card is driven into the guide by a micrometer which is spring loaded to eliminate backlash.

A number of materials were tried as attenuation elements in an attempt to obtain the maximum attenuation over the band with the minimum frequency sensitivity. These include NARDA IRON, Synthane and Filmohm. The material which gave the best results was 180 Ω per square Filmohm. A calibration curve for the attenuator is given in Figure 26. A curve of the maximum VSWR over the band is given in Figure 27.

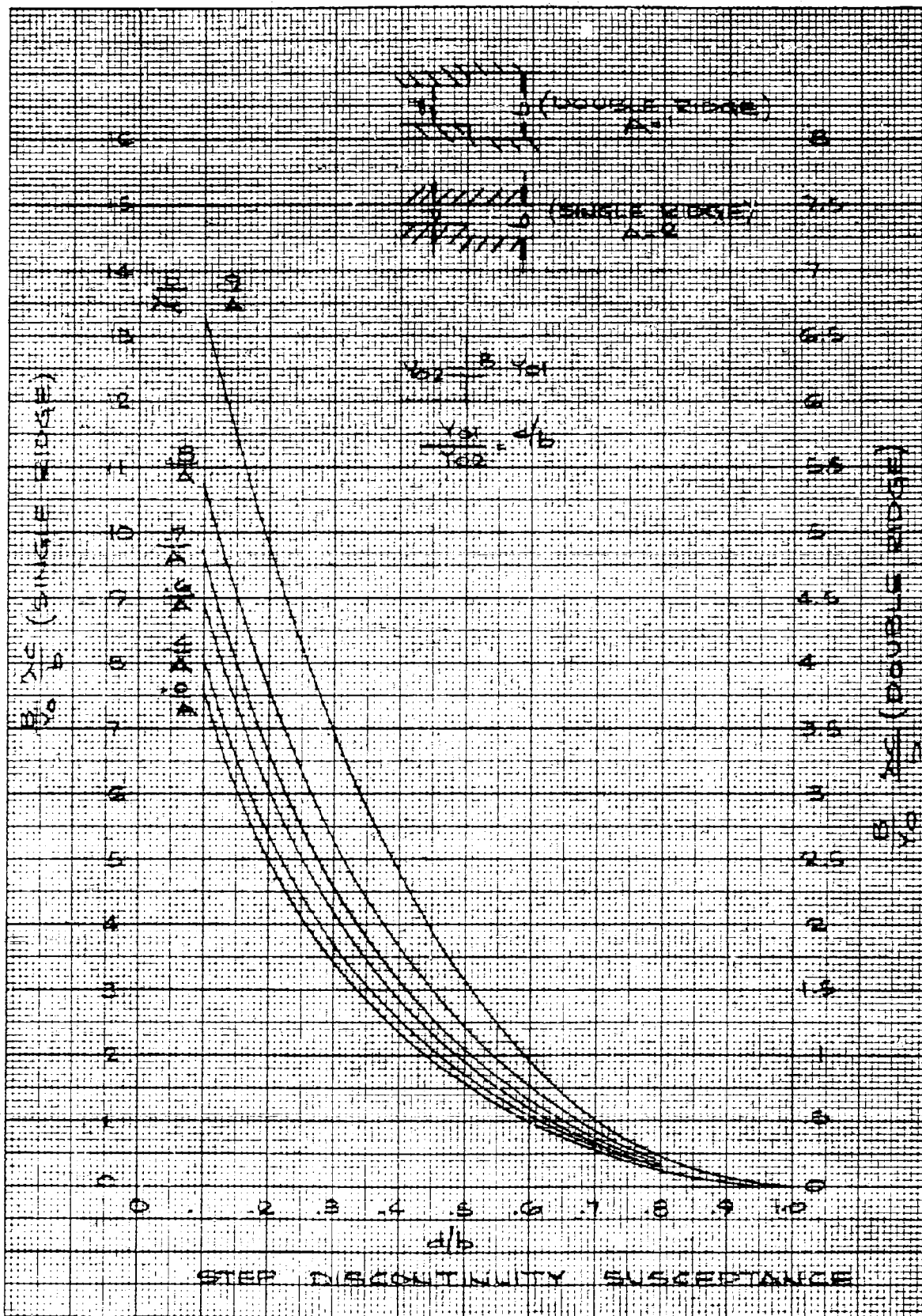


FIG. 25

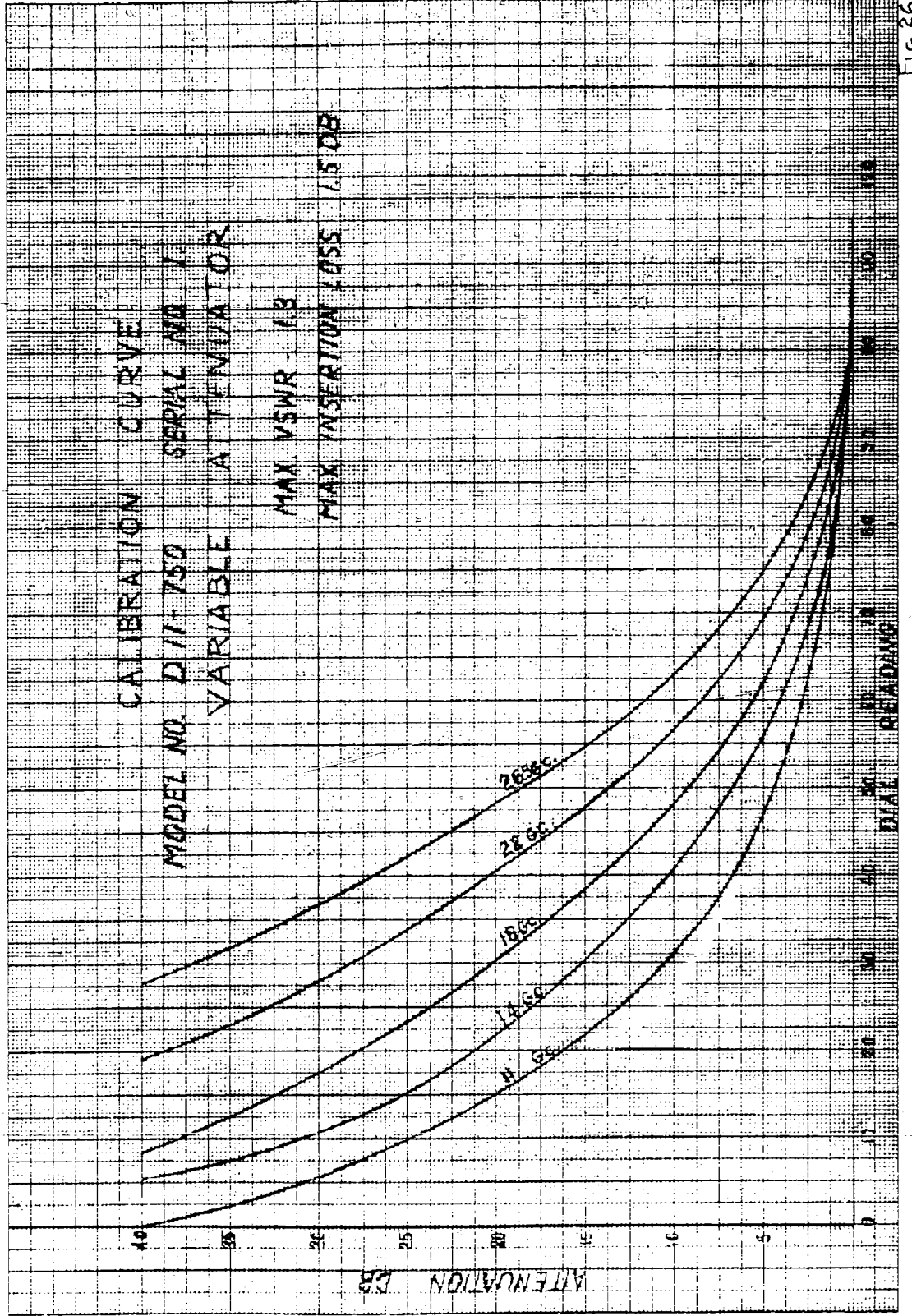


FIG. 26

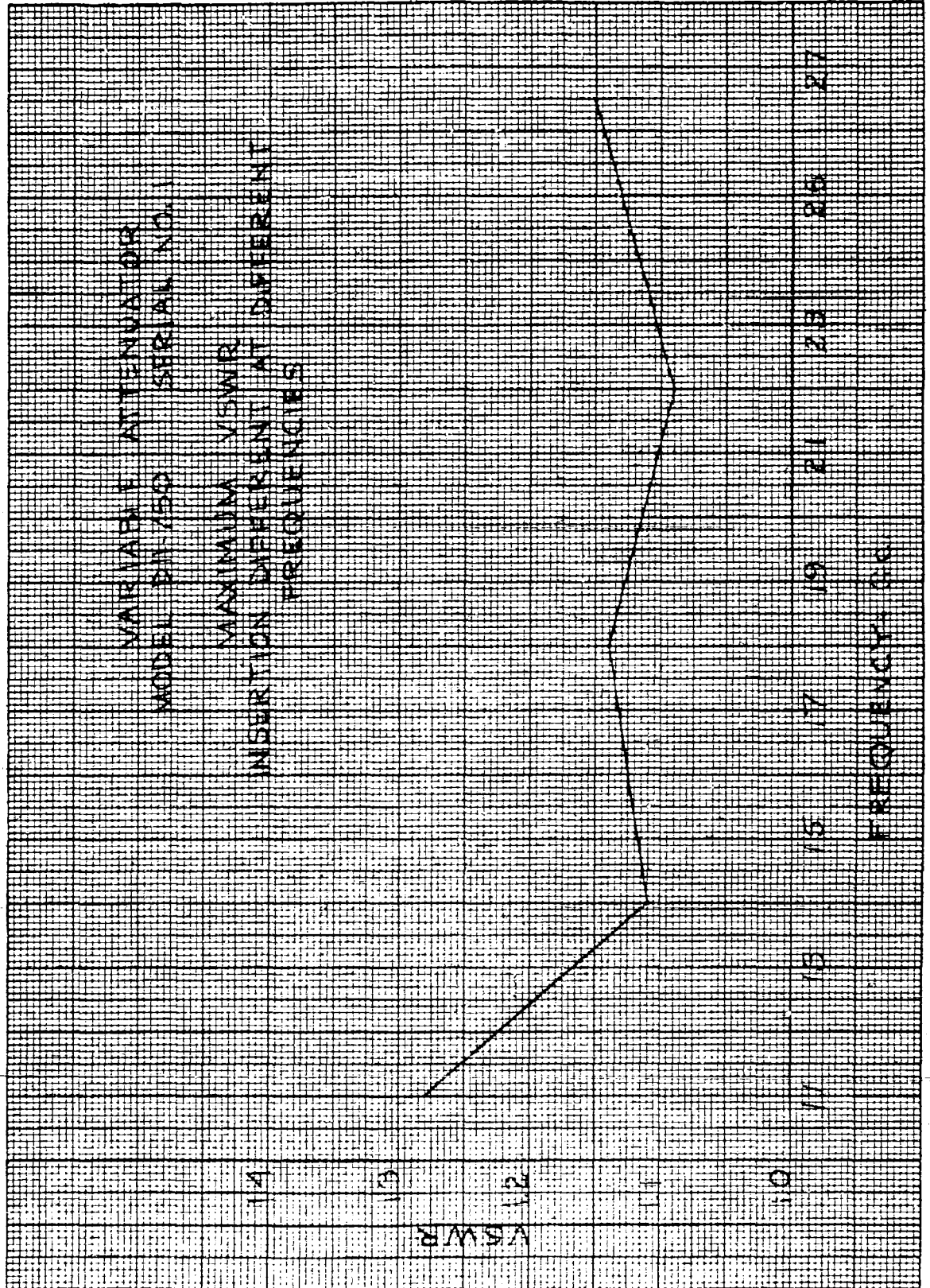


Fig. 27

E-H Tuner

An E-H tuner was built in the form of a four port junction of double ridge waveguide E and H plane tee sections (Figure 28). Due to the geometry of the junction, continuity of the double ridge can only be preserved in one plane (Figure 29). It was decided to preserve the ridge continuity in the E plane tee both for mechanical reasons and because the introduction of an H-plane ridge at right angles to the main line would create a large discontinuity in the transmission path. The ridges in the H-plane arm were therefore terminated at the side wall of the main line guide (see Figure 30).

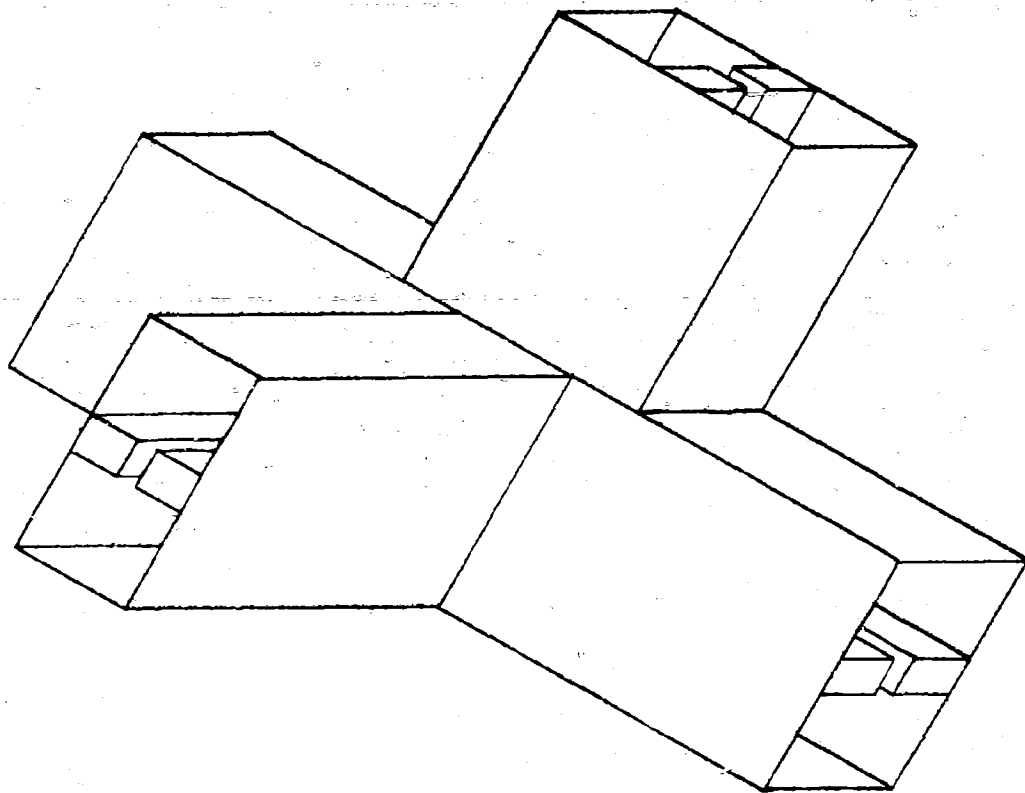
As a preliminary step in the development of this tuner, a test piece was built in the D9 (4.75 - 11 Gc) waveguide size using the available extruded aluminum double ridge tubing and a pair of sliding shorts which were developed under the previous contract (DA 36-039 SC 78187)³.

The data obtained from this test piece was sufficiently encouraging to justify the design of a similar structure in the D11 size. All waveguides in D11 were formed by precision machining from solid aluminum bar stock.

During the tests of the D9 unit, it was noted that the coupling to the H-plane side arm was not tight enough for satisfactory tuning of the H-plane short. This was attributed to the termination of the H-plane ridges at the side wall of the main line. It was obvious that some sort of coupling structure had to be designed to compensate for weak coupling to the H-arm.

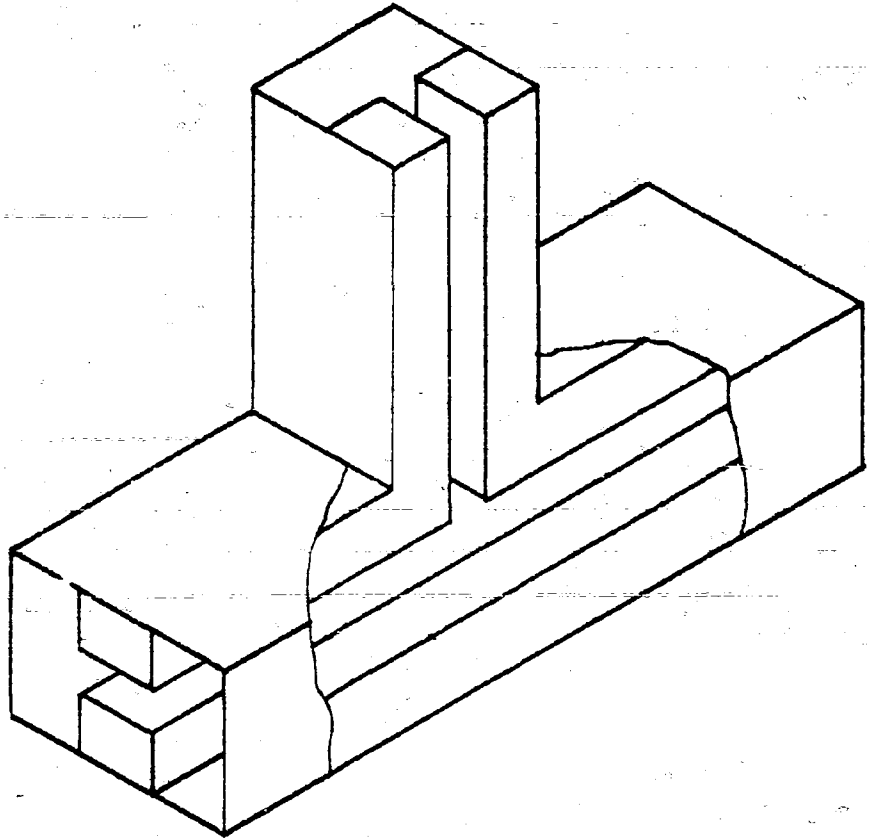
³

See Reference 1



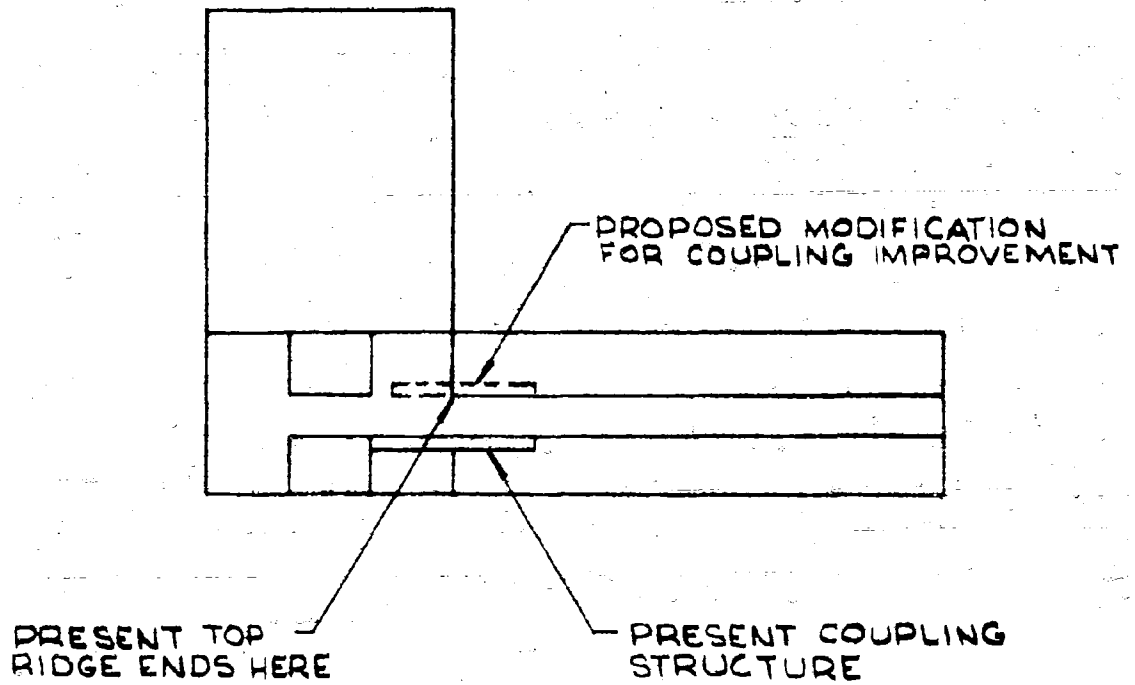
E-H TUNER Showing Junction and Orientation
of Waveguides

Fig. 28



E-H TUNER Showing Continuity of Double Ridge
in E-Plane

Fig. 29



End View of E-H TUNER Showing H-Arm Coupling

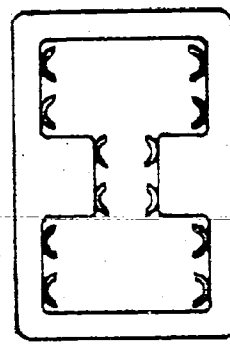
Fig. 30

A number of coupling structures, in the form of thin metallic plates from the lower ridge in the side arm to the lower main line ridge, were designed and tested in order to improve the coupling to the H-arm. The present form (see Figure 30) is the best compromise between side arm coupling and main line VSWR. A main line discontinuity would limit the best obtainable match. It is believed that further improvement in coupling could be achieved by adding an additional capacitive coupling structure in the top of the side arm as shown dotted in Figure 30. The present tuner using only lower ridge compensation introduces a VSWR of 11:1 minimum with greater than 20:1 over most of the range.

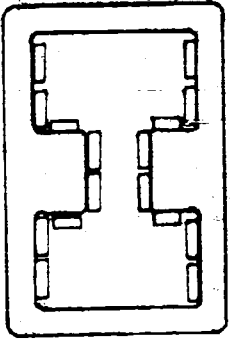
Tunable Waveguide Short

A short was made using positive contact fingers as the shorting mechanism. In the first assembly, commercially available spring fingers were used. These were found to be lossy and erratic since the contact area was limited (see Figure 31a). To remedy this defect, fingers were made by slitting a piece of sheet metal which had been wrapped around the shorting block (see Figure 31b). This modification resulted in a short with smooth performance and a minimum reflection coefficient of 0.97, corresponding to a VSWR \geq 37 db across the band as shown in Figure 32 .

The short is tuned by means of a non-rotating micrometer which can be read to 0.001 inch. The minimum travel is greater than 1/2 guide wavelength at the lowest frequency in the band.



Commercial Spring Fingers
(a)



Final Design Fingers
(b)

TUNABLE WAVEGUIDE SHORT

Fig. 31

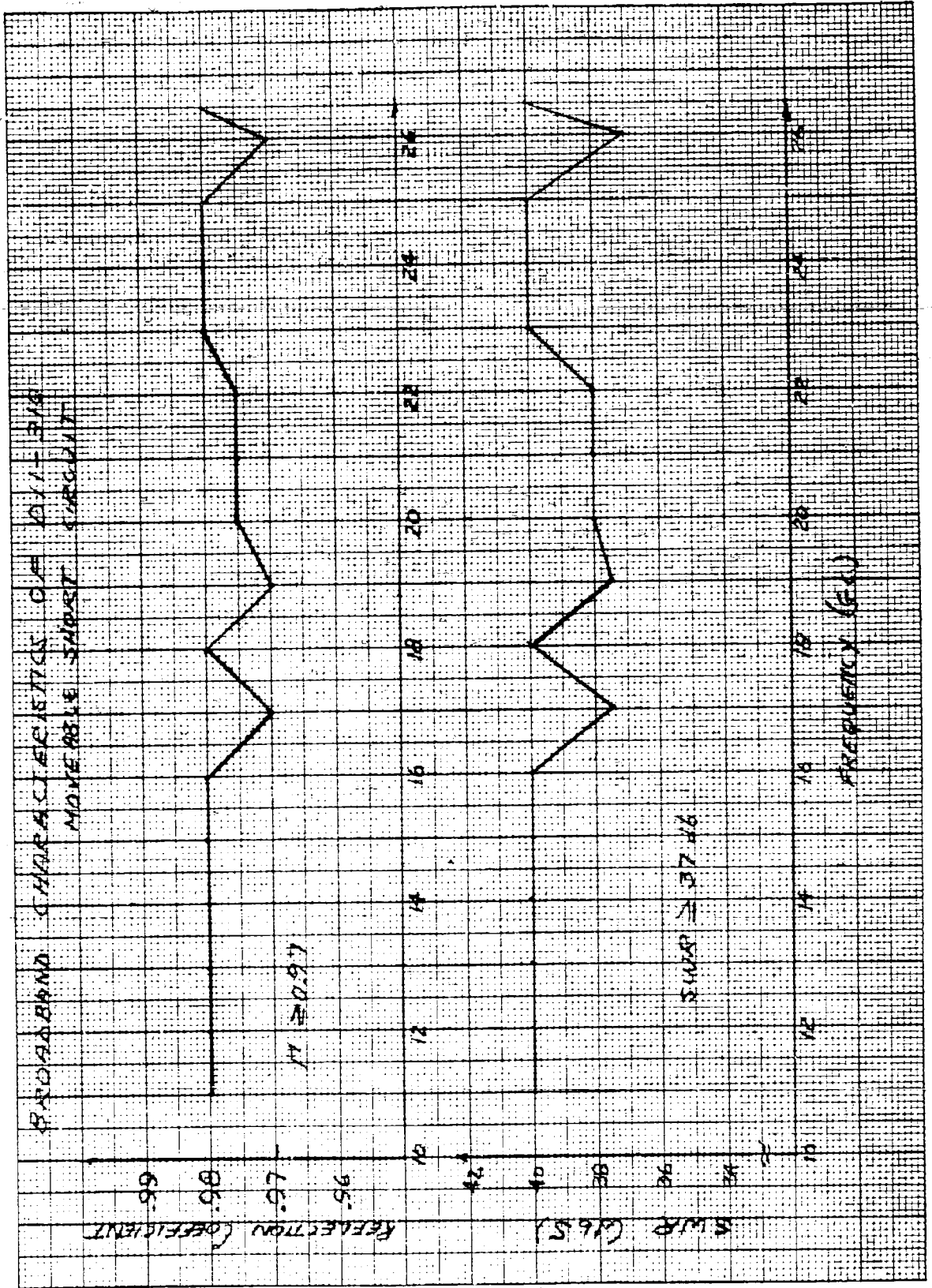
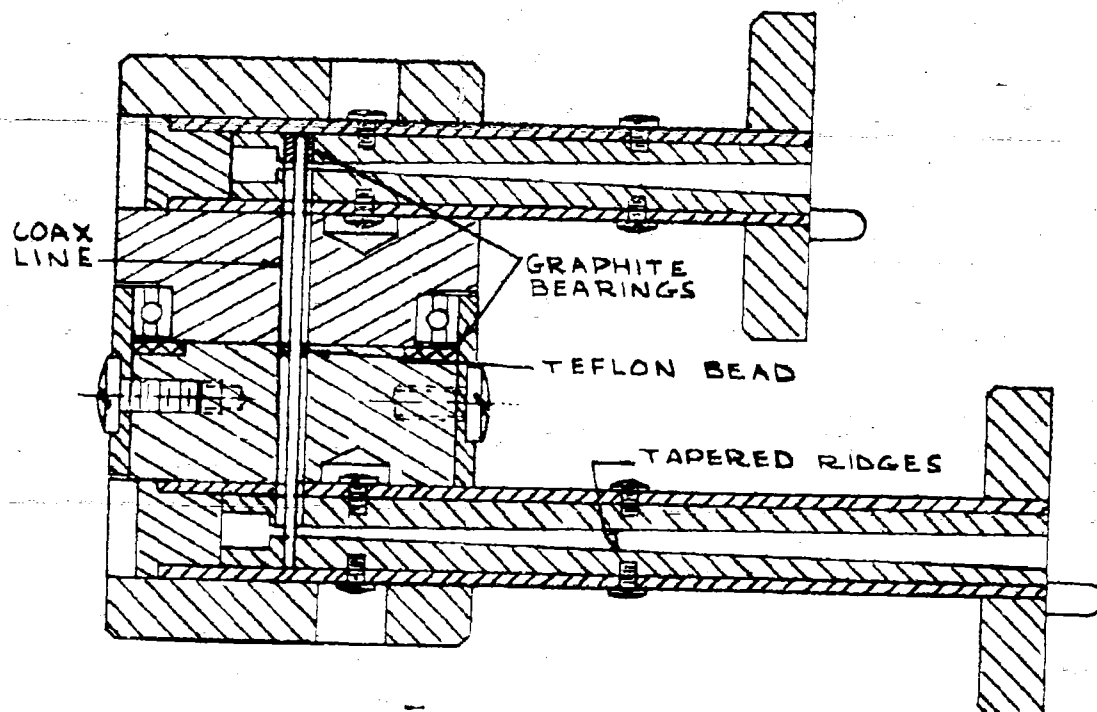


Fig. 32

Rotary Joint

The rotary joint is used primarily to transfer power from a source to a rotating antenna. The joint made for this contract consists primarily of double ridge guide input and output arms with transitions to a rotary coaxial section (see Figure 33). The ridges in each arm taper from the standard ridge guide dimensions to a cross section with a 50Ω characteristic impedance in order to match to a 50Ω coaxial line. The dimensions of the coaxial line are limited by the ridge width since the line must pass through the ridge. The center conductor must be heavy enough to withstand the torsional forces imposed on it. Considering these factors, a coaxial line with an outer diameter of 0.082 and an inner diameter of 0.032 were chosen, giving a characteristic impedance of 50Ω . The attenuation of coaxial lines at 26.5 Gc is high compared to what it is at frequencies where coax is normally used. For the particular line used, the attenuation is .31 db/in. The length of the coaxial section must be at least one inch to allow for clearance of components when rotating, so that the insertion loss will be at least 0.3 db. The VSWR of each coax to ridge guide transition was optimized separately using a special lossy NARDA IRON coaxial termination. The transitions are different. In one the center conductor is solidly fixed into the ridge while in the other the center conductor is free to rotate within a bearing. The bearing consists of a Graphite bushing within which the center conductor rotates with a sliding fit assuring electrical contact (see

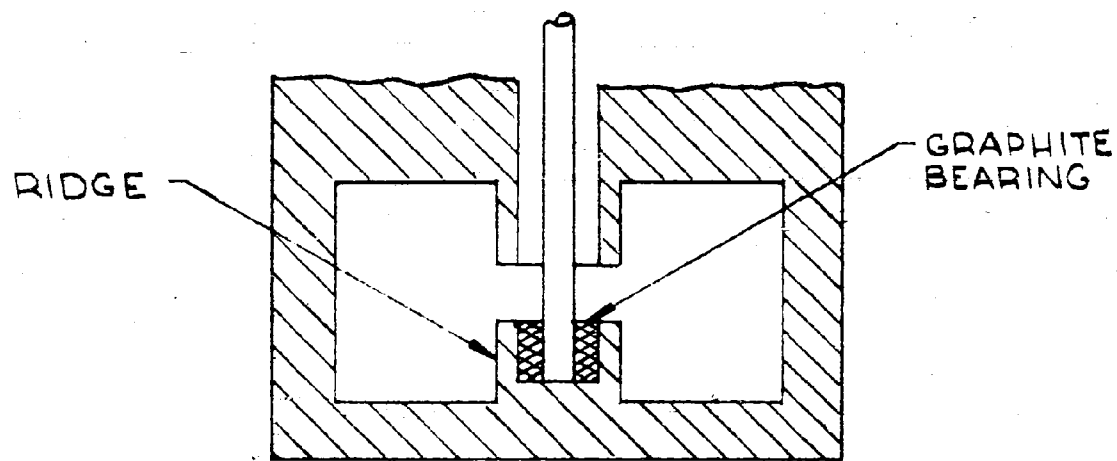


DOUBLE RIDGE GUIDE ROTARY JOINT

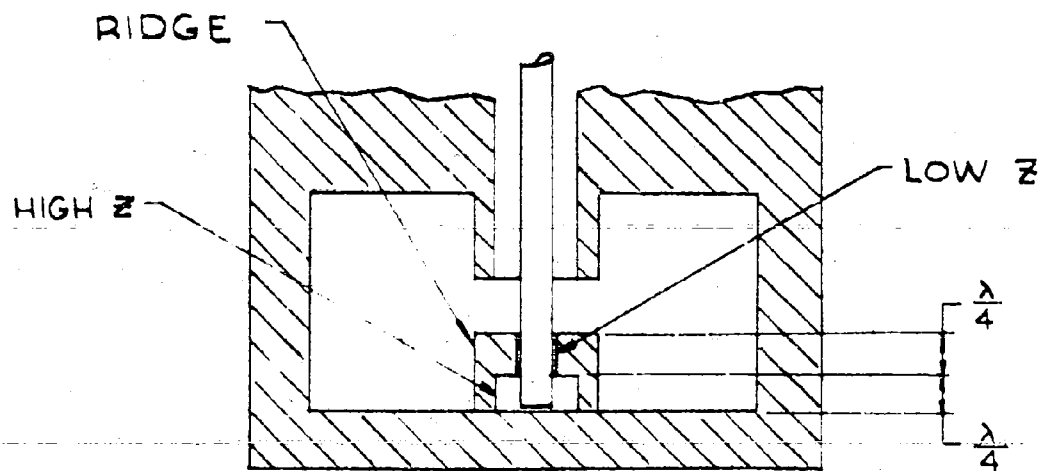
Fig. 33

Figure 34a). In attempting to reduce the insertion loss this bushing was replaced by one made of Teflon dielectric. However, no significant difference was observed. Another method of accomplishing rotation would be with a non-contacting choke section (See Figure 34b) within which the center conductor would turn. Time did not permit attempting this approach. However, this might be one method of reducing the insertion loss. The VSWR of each section was optimized by varying the length of the back cavity dimension. A maximum VSWR of 1.6 was obtained in each section. The sections were assembled with a Graphite bearing in the center (see Figure 33) A short low loss dielectric bead was used to prevent the center conductor from bowing. The results obtained with this configuration are shown in Figure 35 . Maximum VSWR was 2.51, and maximum insertion loss was 1.5db. The required VSWR of 1.25 for this component is considered unrealistic. Neglecting other factors, the maximum VSWR due to the coaxial transitions might be $1.6 \times 1.6 = 2.56$. This will give a reflected loss of 0.76 db. Adding the coaxial line loss will give a total insertion loss of 1.07 db. It does not seem possible to substantially improve the VSWR of the transitions, since the best results with the coaxial to ridged guide transition in the 4.75 to 11.0 Gc band gave a 1.5 VSWR. One proposed method of improvement is to vary the coaxial line length between the transitions to effect some cancellation in the VSWR due to phasing of the mismatches.

Line lengths may be altered by either a physical change in length



Final Design
(a)



Possible Choke Design
(b)

Fig. 34

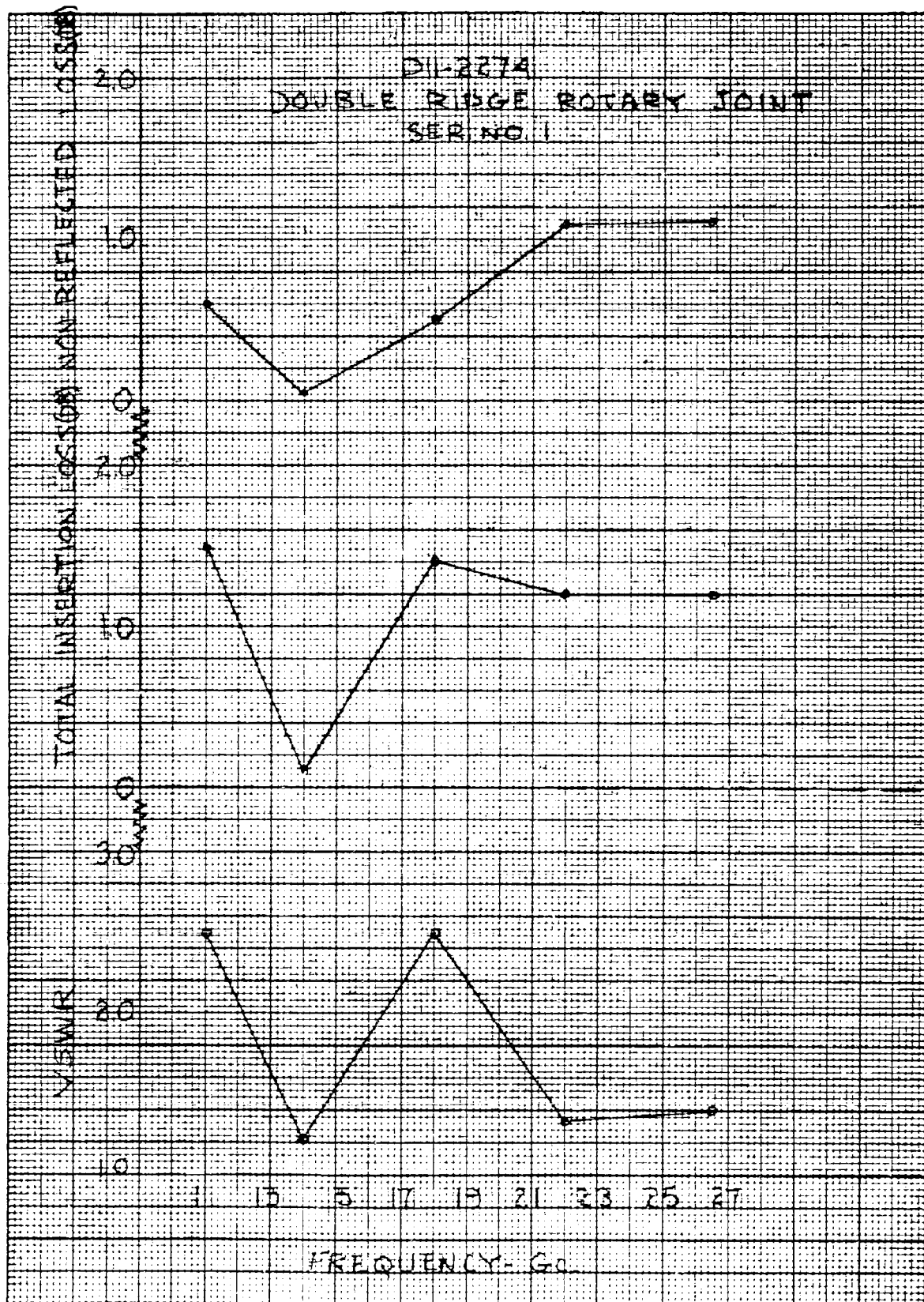


Fig. 35

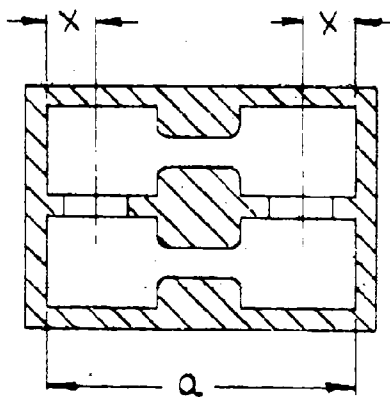
or by dielectric loading to change the electrical length. Dielectric loading was found to increase the insertion loss.

This method was tried to a limited extent during the contract. The extent of work done was not conclusive. Time and funding were factors limiting the scope of work done on this particular parameter.

A number of other attempts were made to try to reduce VSWR and insertion loss. These included using a thin dielectric sheet as an outer conductor bearing, instead of a Graphite center conductor bearing, eliminating the dielectric bead center conductor support and building in a choke section in the outer conductor gap. The choke section was eliminated from consideration in the original design since it was calculated that extraneous modes could be set up if perfect symmetry was not maintained. All of the modifications which were tried could not effect an improvement so that the original design was retained.

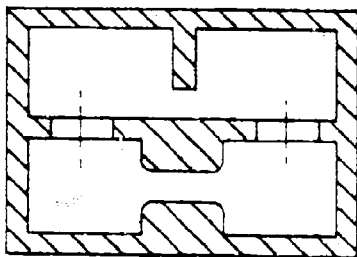
Directional Coupler

The present directional coupler was made using iris coupling between two identical waveguides as shown in Figure 36a . This differs from the coupler made in the 4.75 to 11.0 KMC range which had a single ridge secondary line as shown in Figure 36b . It was possible to use the single ridge configuration for the secondary line in that frequency range since the secondary line output used a transition from the single ridge guide to coaxial line. In the 11.0 to 26.5 KMC range it is not practical to use coaxial line because of the high loss at these frequencies. Therefore, the secondary line in this case must come out in double ridge guide.



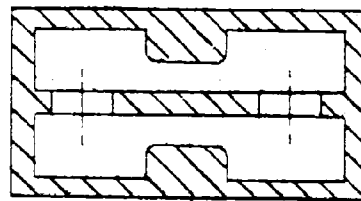
Double to Double Rounded
Ridge Configuration

(a)



Double Rounded to Single
Square Ridge Configuration

(b)



Single to Single Rounded
Ridge Configuration

(c)

RIDGE GUIDE
Directional Coupler Configurations

Fig. 36

Another possible configuration is shown in Figure 36 c . Double to single ridge transitions are made in the primary and secondary lines. The unridged coupling hole plate allows greater variation in the position of the coupling holes in relation to the guide walls. In the double to double ridge configuration it was found that the holes should be closer to the guide center for flatter coupling. Because of the ridges, this was impossible to achieve. The single to single ridge configuration will overcome this difficulty. However, it was determined that the mismatches from the double to single transition and the machining difficulties involved make this approach undesirable.

A sample calculation for determining the coupling values for each hole in the Tchebyscheff pattern is given in Appendix B. The hole diameter required to give a particular coupling is determined experimentally by making test patterns consisting of holes of the same diameter a particular distance from the side wall. A plot of hole diameter vs coupling per hole is given in Figure 37 , for the optimum hole location, which was found to be $x = 0.093$. The optimum spacing between holes which gave the best directivity is 0.1925 . A plot of coupling, directivity and VSWR is given in Figure 38 . The average coupling was 19.85 db with a variation with frequency of ± 3.55 db. The directivity was a minimum of 29 db. VSWR was 1.07 or less in both the primary and secondary lines.

Balanced Mixer

General: There are a number of characteristics which justify the design of a balanced mixer rather than a simpler single ended mixer.

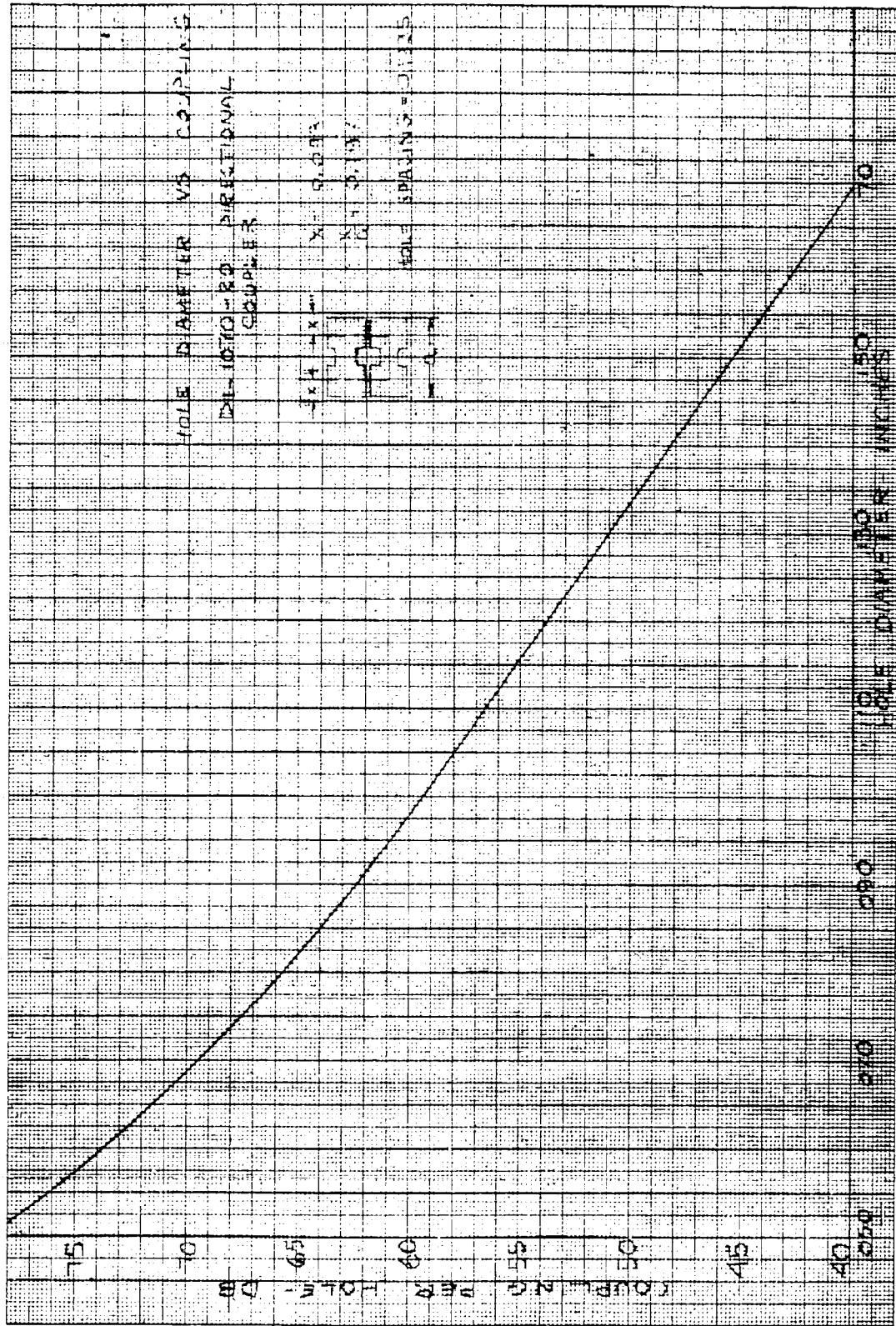


FIG. 37

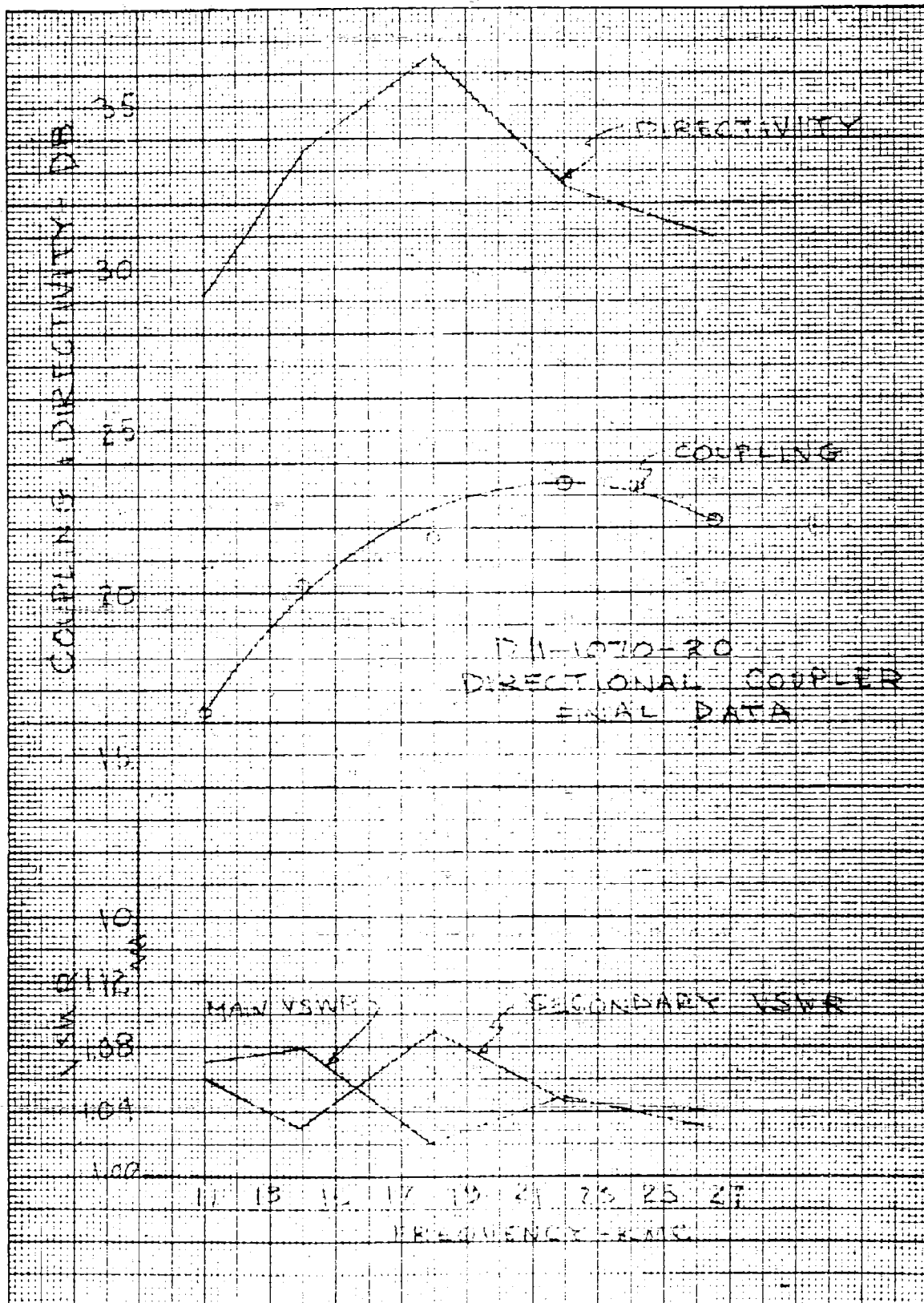


Fig. 38

The most obvious advantage is local oscillator (L.O.) noise suppression, but there are others in the form of L.O. and signal circuit isolation, and lower L.O. power requirements.

A low value of required L.O. power is extremely desirable because sources capable of broadband operation have limited power output. Fixed broadband coupling to the L.O. is desirable to allow for rapid tuning of the receiver, which is necessary since the mixer is to operate over the entire D11 band. Isolation is desirable to limit radiation of L.O. power from the antenna which is connected to the signal port, and also eliminate possible L.O. frequency pulling by reactances in the signal circuit.

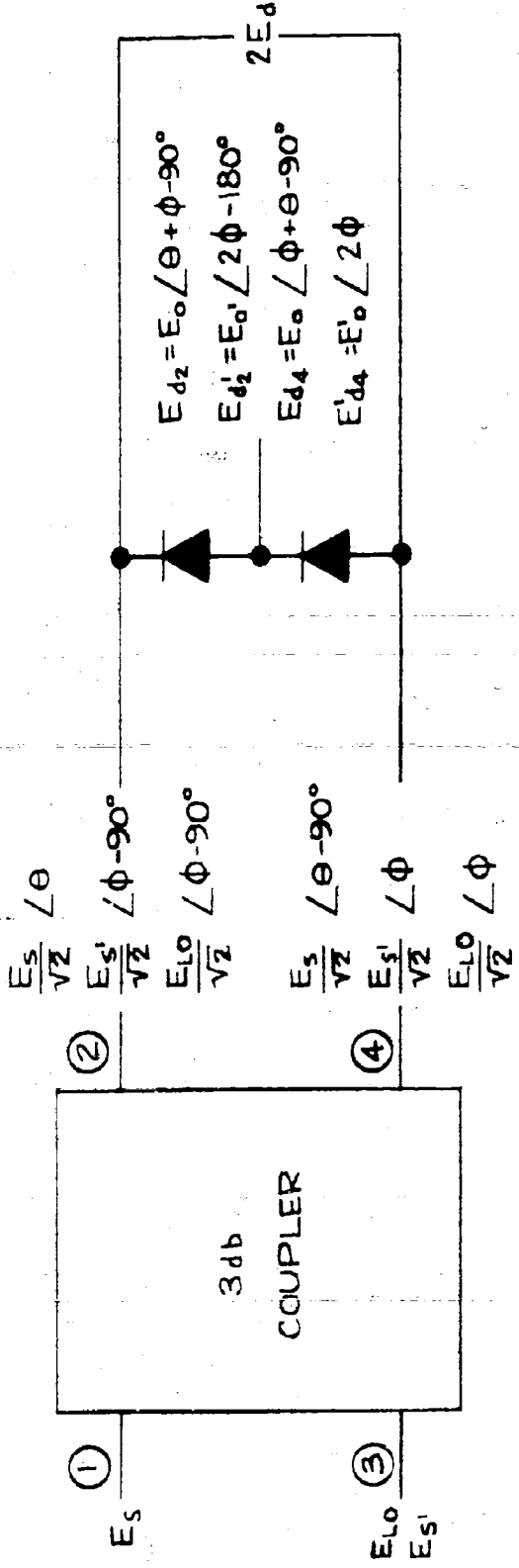
Two basic configurations for a balanced mixer were investigated under this contract. The first method was the 90° coupler mixer.

90° Coupler Mixer

Theory of Operation

This mixer incorporates a hybrid junction in the form of a sidewall coupled-3 db directional coupler as the mechanism by which signal and L.O. powers are combined.

This device is shown schematically in Figure 39 . Signal voltage E_s is introduced at port 1 and divides evenly between ports 2 and 4. There is a relative phase shift of 90 degrees between these ports and the phase delay through the coupler is 6 degrees. Local oscillator voltage E_{LO} and the signal frequency



PHASE RELATIONS IN THE 90° MIXER

Fig. 39

component of L.O. noise voltage E_{g1} , are introduced at port 3, dividing evenly between ports 2 and 4 as shown. Mixer crystals are placed at ports 2 and 4. The I.F. voltages E_{d2} and E_{d4} produced by the crystal convertors have a relative phase shift between them at ports 2 and 4 which is determined by the sum of phase shifts at the two frequencies from which they are derived. Thus the difference frequency at port 2 due to the true signal voltage E_s and the local oscillator voltage E_{LO} is $E_d = E_0 \angle \theta + \phi - 90^\circ$ while the IF voltage due to L.O. noise voltage E_{g1} and L.O. voltage E_{LO} is $E'_{d2} = E'_0 \angle 2\phi - 180^\circ$.

The net effect is to produce in-phase IF voltages at ports 2 and 4 for the IF voltage derived from mixing L.O. and signal power. The IF voltages due to mixing of L.O. and L.O. noise powers result in reversed phase components at the two ports.

The crystals are series connected between ports 2 and 4, so that the in-phase components add and the reversed phase noise components cancel. The series connection is obtained either by using reversed polarity crystals or by using normal crystals in reversed mounts. The former procedure is preferred for mechanical simplicity since the crystals are purchased and their polarity is easily reversed during manufacture; while reversing the mount polarity requires involved design work.

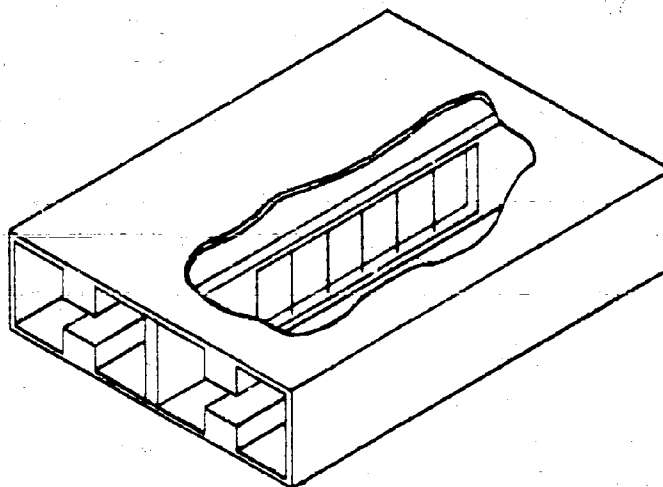
The same results are obtained if the input contains sideband components at the L.O. frequency. These undergo the same phase shift as the desired signal and are cancelled in the mixer.

The first attempt at a double ridge balanced mixer was to be of the 90° coupler type. The justification for this lay in the fact that some experience with multihole couplers in ridge waveguide was available and a 20 db coupler was already under development as part of the project. Data taken in the 20 db coupler program made it apparent that a balanced 3 db hybrid was unattainable using multi-hole coupling.

A search was therefore made to locate a coupling mechanism that was capable of flat coupling over a broadband. Another coupling mechanism was tried⁴ which utilized warped mode coupling of waves in sidewall coupled waveguides. The coupling was obtained through a wire grating which filled the aperture between the two guides. Experimental evidence had shown that a coupling of $4 \text{ db} \pm 0.15 \text{ db}$ over a 10% bandwidth was obtained in rectangular waveguide with no compensation for changes in guide wavelength variation and the discontinuity caused by the array.

Reference 10 indicated that if compensation were applied, the useful bandwidth could be greatly extended. The best results with a test coupler using this grid array in D9 size extruded ridge waveguide tubing was $3.8 \text{ db} \pm 2.7 \text{ db}$ from 4.75 to 7.50 KMC. It was decided that this technique did not offer possibilities of flat enough coupling over the required band. A sketch of the test piece is shown in Figure 40.

⁴See Reference 10



Sketch of SIDEWALL COUPLED RIDGE GUIDE COUPLER
USING WIRE GRATING

Fig. 40

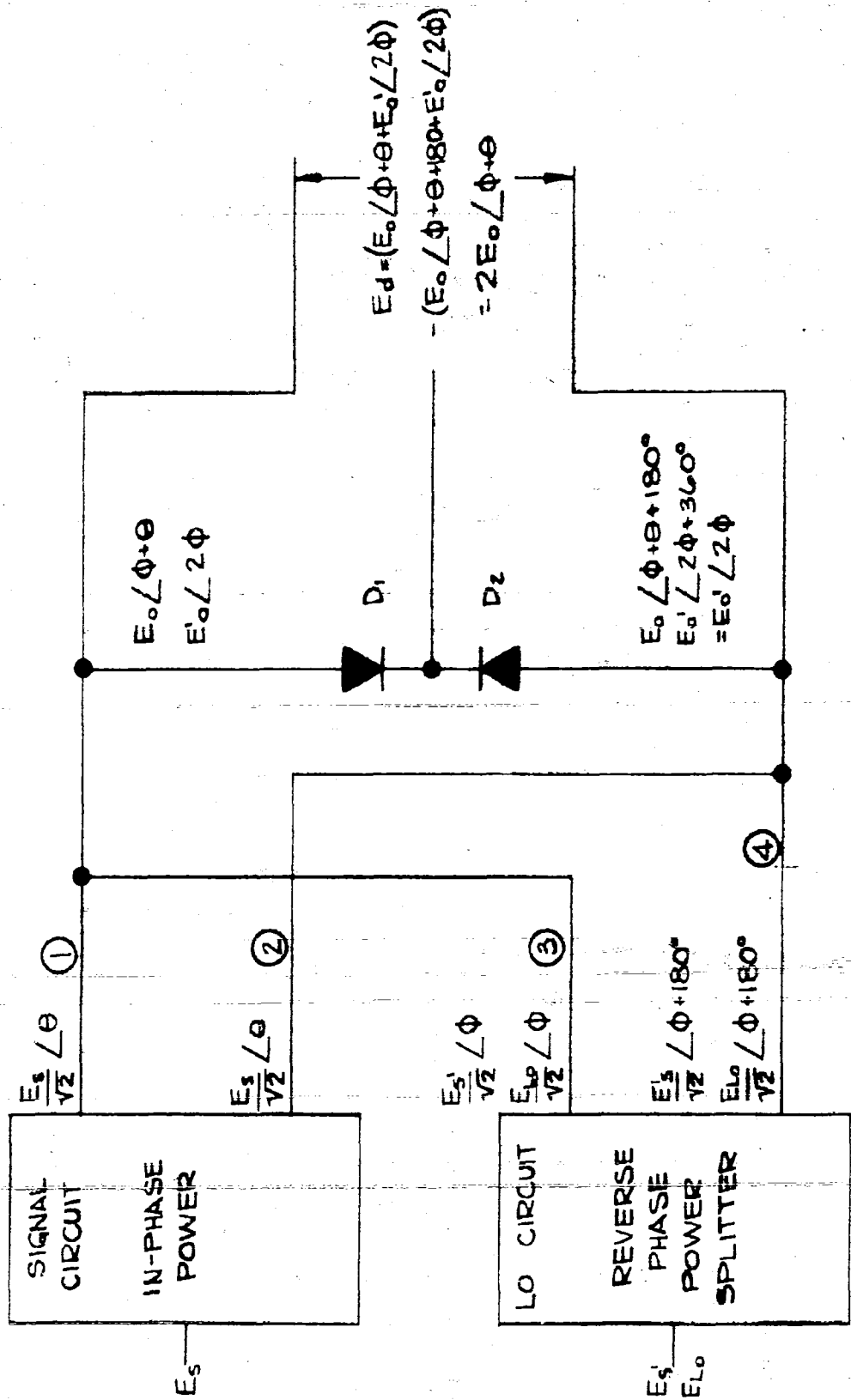
On the basis of the investigation described above, it was decided that development of a broadband coupling structure would require a method which did not rely on frequency sensitive coupling elements. The desired coupler would be a type which gave power division simply on the basis of geometry. The "reversed-field" mixer utilizes this type of coupling and it formed the basis of our second design.

Reversed-Field Mixer

Theory of Operation

The reversed field mixer is composed of an in-phase equal power splitter in the input signal circuit and a reversed-phase balanced power splitter in the L.O. circuit. The L.O. noise suppression of this device can best be explained by reference to the schematic representation of Figure 41.

Signal frequency voltage E_s enters the signal circuit in-phase power splitter, dividing equally ($E_s/\sqrt{2}$) at ports 1 and 2. There is no relative phase shift between ports 2 and 4; but there is a phase delay (θ) from the input to each of the outputs. The input to the L.O. circuit consists of a component E_{LO} at the LO frequency and a noise component E_{s1} at the signal frequency. Both of these components divide evenly and appear at ports 3 and 4. There is 180° relative phase shift between ports 3 and 4; in addition to the phase delay (ϕ) from the input to each of the ports. The signals at ports 1 and 3 are combined at one diode (D_1) while those



Schematic Representation of REVERSED FIELD MIXER

Fig. 41

of 2 and 4 are combined at the other diode (D_2). At D_1 two IF components are generated, E_0 and E_{01} ; each having the combined phase of the voltages which produced them. Thus E_0 is produced from signal and LO voltages, while E_{01} is the result of the combination of the L.O. and noise voltages.

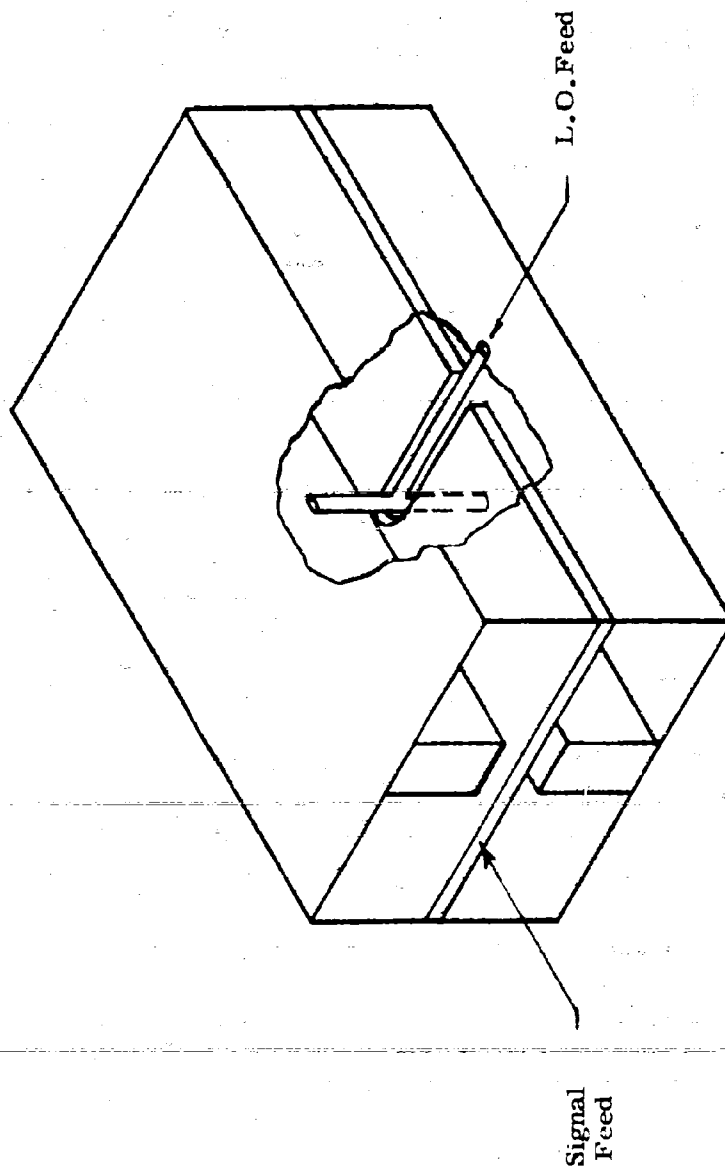
Since the diodes are connected in series bucking, in-phase voltages (E_{01}) cancel while out of phase components (E_0) add; thus the output of the mixer does not contain any extraneous information due to noise components present in the L.O. source output.

Due to symmetry sidebands of the input signal at the L.O. frequency are also cancelled.

A reverse phase mixer was constructed in double ridge waveguide using an H-plane septum as the in-phase power splitter in the signal circuit, and an E-plane coaxial tee tuned to provide reversed phase equal power signals from the local oscillator. The physical configurations of these couplers are shown in Figure 42; while the fields that they set up are shown in Figure 43.

The mixer diodes have a common connection through the septum to their respective pin terminals. A matched pair of diodes is used to facilitate balance.

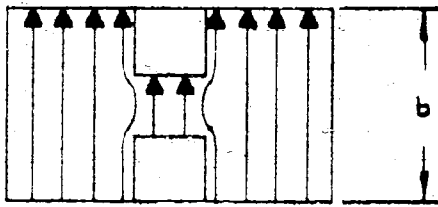
Although the L.O. feed is in coaxial line, a waveguide input is provided. An integrally built ridge guide to coax transition is used for this purpose. The crystals are fed from the coax end of a wave-



Coupling section of REVERSED PHASE MIXER showing signal and L.O. power splitters

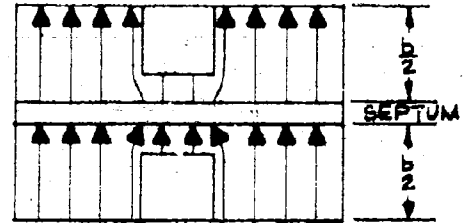
Fig. 42

ELECTRIC FIELD CONFIGURATIONS FOR RIDGE GUIDE STRUCTURES



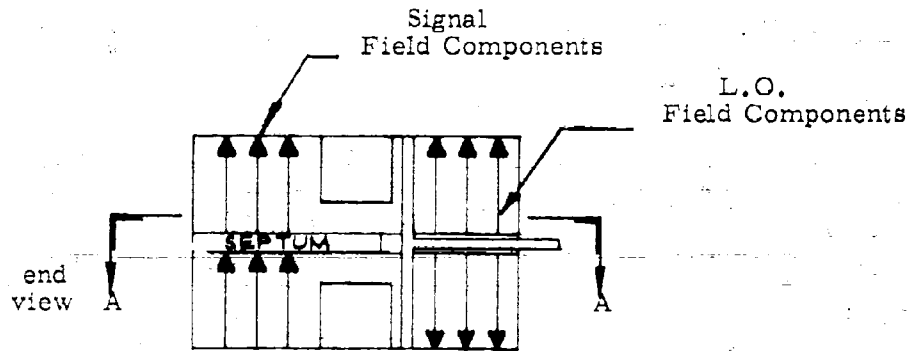
Normal Double Ridge Guide

(a)



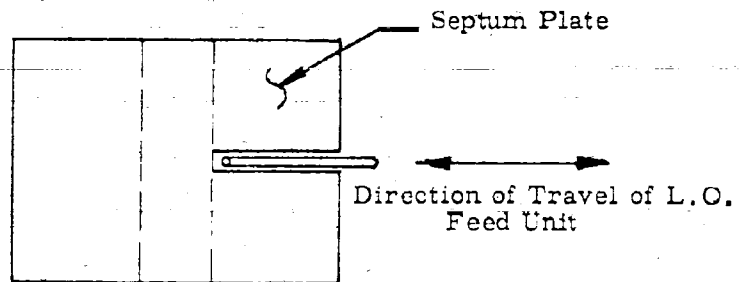
Ridge Guide with H - Plane Power

(b)



Coaxial Tee Field Reversed Phase Power Splitter

(c)



Coaxial Tee-Feed - Top View (Section A-A of Fig. 43 (c)) showing construction

Fig. 43

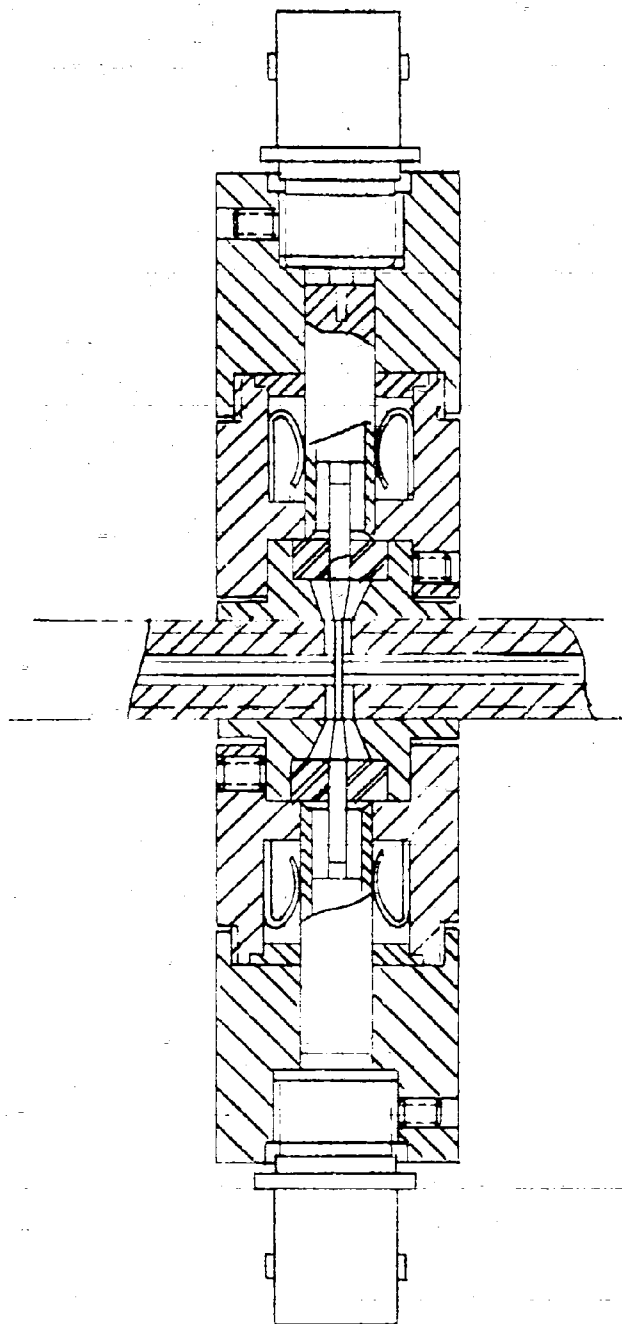
guide to coax transition. The L.O. feed is shown in Figure 42, and the crystal feed is shown in Figure 44.

Tuning adjustments are provided on the experimental model for purposes of taking data under a variety of conditions. Each of the waveguide to coax transitions is equipped with an adjustable short in the cavity behind each transition. The shorts for the crystal transitions are single ridge to fit the single ridge guide formed by the H-plane septum. Another adjustment is available through variation of position of the "tee-bar" L.O. feed across the width of the main line.

The present mixer is a developmental model which has not been fully developed due to limited funds. A number of modifications still remain to be made before a satisfactory unit is achieved. However, enough data has been taken to prove out the basic design configuration.

Tests were made at mid-band (18.0 Gc) and the two end point frequencies (11.0 and 26.5 Gc). Excellent balance was obtained with only slight adjustments of the separate crystal mount shorts at all three frequencies.

Coupling from the L.O. circuit was -20 db(minimum) at 11 Gc; and -14 db at 18 Gc. The coupling value at 26.5 Gc could not be determined due to measurement problems. This situation results from loading effects of the discontinuities in the mixer



SIMPLIFIED SKETCH OF CRYSTAL MOUNT
FOR DII-BALANCED MIXER

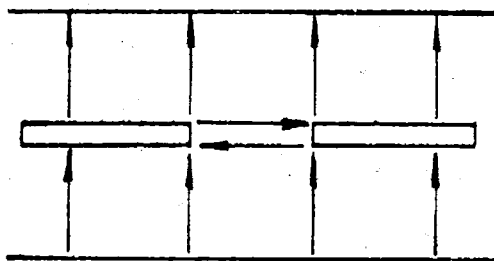
Fig. 44

structure; particularly those due to the discontinuity at the leading edge of the H-plane septum. A method by which this effect could be neutralized has been considered.

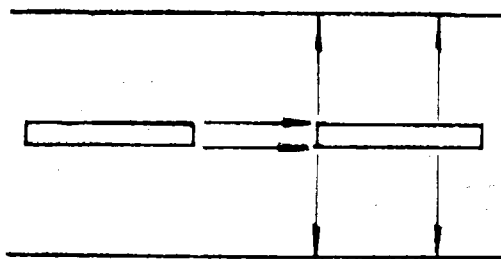
The neutralizing structure would take the form of a transverse slot in the septum plate. A side view of the plate and slot is shown in Figure 45. The in-phase E field components from the signal port pass the slot undisturbed since they produce a net zero field across the slot; the slot appears as a series short circuit (Figure 45a). For the reversed E fields due to L.O. input (Figure 45b) there is a net field across the slot which appears as a series open circuit. This series open circuit appearing close to the L.O. feed imposes a high impedance load to the L.O. for any line length between the L.O. feed and the septum. An optimum position of the slot would have to be determined empirically.

In view of the good results obtained at the low and mid-band frequencies, it is expected that satisfactory coupling at the high end of the band could be obtained through further development.

Isolation was found to be greater than 20 db during all the tests. This result was expected since the power splitters in both the L.O. and signal circuits depend on geometric properties of their respective junctions. Since the isolation is based on geometry, one would expect a constant value independent of frequency. However it was found that the isolation increased from a value of 20 db (min.)



a) Signal Fields; zero net slot field



b) L.O. fields; net slot fields

COMPENSATION FOR SEPTUM DISCONTINUITY

Fig. 45

at 11 Gc to > 35 db at 26.5 db. This variation is explainable through a consideration of the frequency dependence of the asymmetric discontinuities in the coupling junctions.

A reasonable amount of diode sensitivity was observed throughout the tests. A minimum of .55 ma. per channel crystal current was produced from 0.75 mw per channel input power.

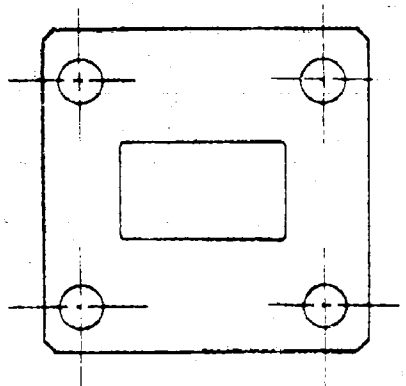
The signal port VSWR was found to be $< 2:1$ at 11 Gc; 5.8:1 at 18 Gc; and 3.5:1 at 26.5 Gc. A maximum figure of 3:1 across the band would be considered good performance. The higher VSWR is partly due to the tapered septum transition from full height double ridge guide to twin single-ridge half-height guide.

The L.O. port VSWR was found to be rather high. This situation is not unreasonable when one considers that the VSWR results from the combined effects of the "tee-bar" feed discontinuity and the reflections through the waveguide to coax transition. The VSWR was found to be 10:1 at 11 Gc; 8:1 at 18 Gc; and 7:1 at 26.5 Gc. Some improvement in this VSWR could be obtained by modifying the coaxial feed. A first attempt would be to use a straight section to replace the "tee-bar". The waveguide to coax transition could also be modified to provide a better match by compensating for the fact that the coax portion is terminated in an impedance other than its characteristic impedance.

The limited amount of testing indicates that a satisfactory basic structure for a ridge guide balanced mixer has been developed. It is believed that further development will lead to either a single unit or at most two units which will operate as balanced mixers across the 11-26.5 Gc band.

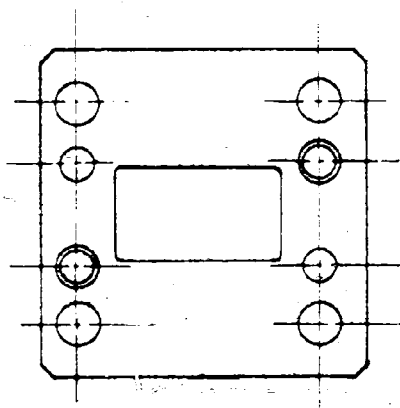
Flanges

Six standard flanges were supplied as part of the contract as shown in Figure 46a . The pins and pin holes are located as shown in Figure 46b . The pins and pin holes must be located accurately with respect to the internal waveguide dimensions to insure proper mating of the waveguide openings. This must be done after securing the flange to the waveguide wall and flange cut out. The pins and pin holes are therefore not included on the flanges. These flanges are being standardized by the Electronic Industries Association for use with standard waveguide tubing; whenever the tubing becomes available. Charts are presented in Figures 47 to 49 giving dimensions for a series of flanges for double ridge 2.4:1 bandwidth waveguide.



DOUBLE RIDGE GUIDE FLANGE

(a)



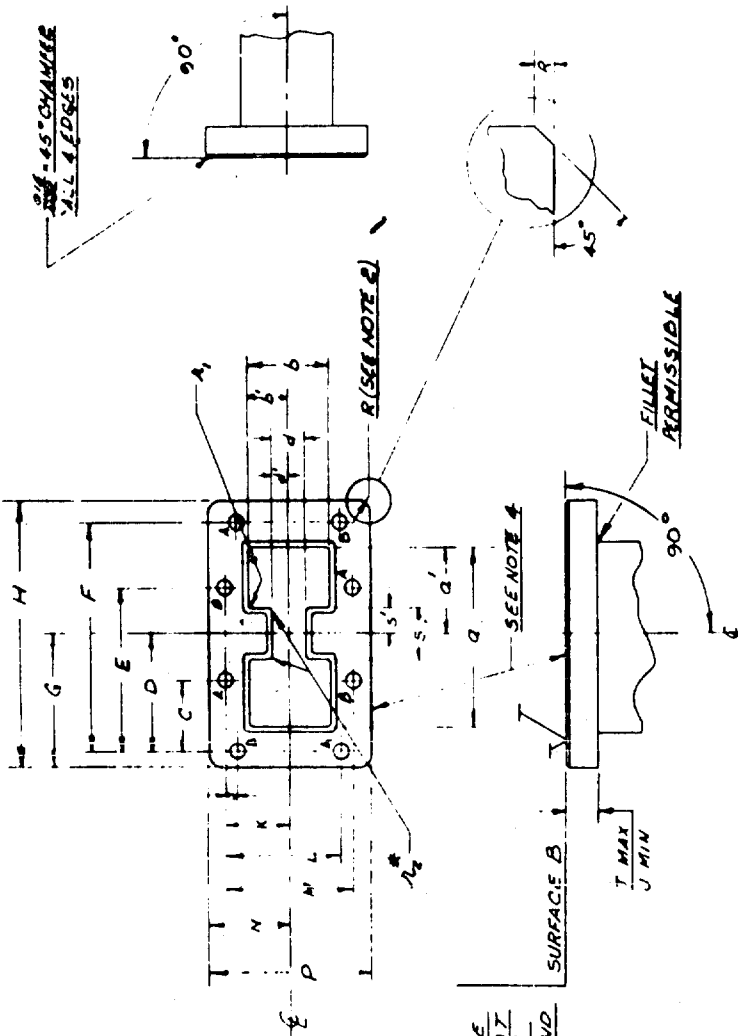
DOUBLE RIDGE GUIDE FLANGE

Showing Pin Locations

(b)

Fig. 46

90° CHAMFER
ALL EDGES



THIS SURFACE
SHALL BE FLAT
WITHIN .001"
(SEE TABLE AND
NOTE 3)

FILLETT
PERMISSIBLE

90°

T MAX
U MIN

SEE NOTE 4

R (SEE NOTE 2)

DIMENSIONS IN INCHES

QWV NO.	QWV RANGE	A	B	C	D	E	F	G	H	I	J	K	L	M	N	P	Q	R	S	T	U	X
00-204	2.0 - 4.0	1.250	1.205	1.295	1.000	1.043	1.043	1.043	1.043	1.043	1.043	1.043	1.043	1.043	1.043	1.043	1.043	1.043	1.043	1.043	1.043	1.043
00-205	4.0 - 8.0	1.480	1.480	1.740	1.344	1.344	1.344	1.344	1.344	1.344	1.344	1.344	1.344	1.344	1.344	1.344	1.344	1.344	1.344	1.344	1.344	1.344
00-206	8.0 - 11.0	1.090	1.090	1.550	1.250	1.250	1.250	1.250	1.250	1.250	1.250	1.250	1.250	1.250	1.250	1.250	1.250	1.250	1.250	1.250	1.250	1.250

- NOTES:
- 1- 'X' PERTAINS TO THE THICKNESS OF THE WHOLE FLANGE FACE INCLUDING END OF WAVEGUIDE.
 - 2- 'R' CORNER RADIUS MAY BE REPLACED AS SHOWN.
 - 3- BEARING SURFACE OF SURVEY COUNTERBORE ALL HOLES ON MATING SURFACE.
 - 4- DEGREE OUTSIDE EDGES ONLY. DO NOT FORM EDGES AT WAVEGUIDE CORNER.
 - 5- .001" TOLERANCE ±10%.
 - 6- 'T' INDICATES A TOLERANCE OF ±.010.

FIG. 48

00-201

QWV NO.	QWV RANGE	QWV																					
00-201																							

LIST OF MATERIAL

NAME: **ARMATURE UNPRESSURIZED CONTACT FLANGES FOR DOUBLE RIGGED AMPLIFIERS**

QWV NO.: **00-201**

QWV RANGE: **C**

QWV: **00-201**

the narda ELECTRONICS CORPORATION
ROSELAND, NEW JERSEY

III. CONCLUSIONS

All the components required for the 11.0 to 26.5 rounded ridge waveguide were designed and built. Workable components which met or approached the required specifications were developed in most cases. The results obtained with the E-H tuner are satisfactory for most applications although the required specifications were not met. Satisfactory results were not achieved in the case of the Rotary Joint and Balanced Mixer. The difficulties which arose in the development of the Mixer and Rotary Joint were three fold. First, there are inherent difficulties associated with broadband component design matching techniques. This was especially true in the case of the Balanced Mixer. Even a good full rectangular waveguide bandwidth balanced mixer is considered "state of the art". Second; there are additional problems due to the higher frequencies involved, compared to the 4.75 to 11.0 Gc band. In the rotary joint, mode problems and coaxial line attenuation proved to be major design considerations. Third, mechanical problems associated with ridges are a major factor in design. In all the components, tight tolerances are required for satisfactory results. In view of the results obtained in the allotted time, it is concluded that additional effort would result in improved performance for the Rotary Joint and Balanced mixer. The results obtained on all the other components for this contract were quite satisfactory and comparable to results which would be expected in rectangular guide of this size.

IV. RECOMMENDATIONS

The Rotary Joint and Balanced Mixer are key components required for systems. In order to fulfill future needs of the Armed Services for ECM systems NARDA strongly recommends that funding be made available to further develop the Rotary Joint and Balanced Mixer into useable components. The recommended approach for improvement of the Rotary Joint is to make line length changes and further choke designs. In the case of the Balanced Mixer, modification of the local oscillator input circuit and crystal mounts is recommended for improving performance. These approaches are detailed in the section devoted to each component. Further investigation should also be performed to find a practical means of manufacturing waveguide in minimum lengths of two to four feet. Machining methods such as broaching might be employed. Additional investigation of electroforming methods is also recommended. The work conducted in this contract would be a natural starting point for future development and investigation in these areas.

IDENTIFICATION OF KEY PERSONNEL

Adolph Brenner

Microwave Section Head

B.E.E. The City College of New York, 1954
Currently attending Polytechnic Institute of Brooklyn for M.E.E.
1953-1958 Microwave Development Engineer, FXR, Inc.
May 1958 - Oct. 1958 Project Engineer, Polarad Electronics Corp.
Since Oct. 1958, Microwave Section Head, Narda Microwave Corp.

Philip Levine

Project Engineer

B.E.E., The City College of New York, 1958
Currently attending Polytechnic Institute of Brooklyn for M.E.E.
1958-1959, Microwave Engineer, Polarad Electronics Corp.
Since 1959, Project Engineer, Narda Microwave Corp.

Peter D. Lubell

Microwave Engineer

B.E.E., The Cooper Union, 1958
Currently attending Polytechnic Institute of Brooklyn for M.E.E.
1958-1959, Microwave Engineer, Wheeler Laboratories
Since 1959, Microwave Engineer, Narda Microwave Corporation

STAFF HOURS SPENT ON PROJECT

	<u>TOTAL</u> to December 1, 1961
A. Brenner	198.3
P. Levine	1144.0
P. Lubell	1063.8
TOTAL	<u>2406.1</u>

REFERENCES

1. Signal Corps Engineering Laboratories, "Broad Band Ridge Waveguides and Components," Final Report, Contract No. DA 36-039 SC 78187, December 1958 to July 1960.
2. Anderson, T. and Kent, L.I., "Standardization of Ridged Waveguides," Microwave Journal, Vol.4, No.4, April 1961.
3. Hopfer, Samuel, "Design of Ridged Waveguides," IRE Transactions, Vol. MTT-3, No.5, October 1955.
4. Navy Department - Bureau of Ships, "Broadband Waveguide Transmission Systems and Components," Final Report, Contract No. NObsr-39294, July 1947 - August 1949.
5. Signal Corps Engineering Laboratories, "Extremely Broadband Waveguide Components," Final Report, Contract No. DA 36-039 SC 42662, April 1953 - June 1954.
6. Cohn, Dr.Seymour, "Unpublished Notes".
7. Kent, L.I., "The Optimum Design of Multielement Directional Couplers," M.E.E. Thesis, May, 1954, Polytechnic Institute of Brooklyn.
8. Cohn, S.B., "Properties of Ridge Waveguide," Proceedings of the IRE, Volume 35, pp. 783-788, August 1947.
9. Marcuvitz, N., "Waveguide Handbook," Rad.Lab. Series, Vol.10, p.309, McGraw Hill Book Co., 1951

10. Miller, S.E., "Coupled Wave Theory and Waveguide Applications,"
Bell System Technical Journal, Volume 33, pp 661-719, May 1954.
11. Bethe, H.A., "Theory of Side Windows in Waveguides," Radiation
Laboratory Report No.199, April 1943.

APPENDIX A

RIDGE-WAVEGUIDE TO RECTANGULAR WAVEGUIDE TRANSITION
DESIGN PROCEDURE

COMPENSATION FOR b/a RATIO CHANGE CONSIDERED

Information given: input impedance
 output impedance
 maximum VSWR desired
 Tchebyscheff coefficients

Calculating the Tchebyscheff coefficients can be done in the usual manner.⁵ The coefficients are then used to determine the impedance values of each section. Impedance values in turn are used to determine cross section geometry of each section. After all this information is obtained the maximum theoretical VSWR can be calculated for each multi-section ($n = 3, 4, 5, \dots$) transition. On this basis four sections were considered adequate. A sample calculation for the RG-53/U transition is given below.

GIVEN: $Z_{\text{input}} = 207.6$ $Z_{\text{output}} = 397.2$ $\text{VSWR}_{\text{max}} = 1.08$

$$\gamma_1' = 1 = \gamma_5' \quad , \quad \gamma_2' = 3.001 = \gamma_4' \quad , \quad \gamma_3' = 4.127$$

$$\frac{Z_{\text{output}}}{Z_{\text{input}}} = \frac{Z_{\text{rectangular}}}{Z_{\text{ridge}}} = 1.913 = (Z_1') \sum_{k=1}^{k=5} \gamma_k' = 2.129$$

$$Z_1' = 1.913 \frac{1}{2.129} = 1.0549$$

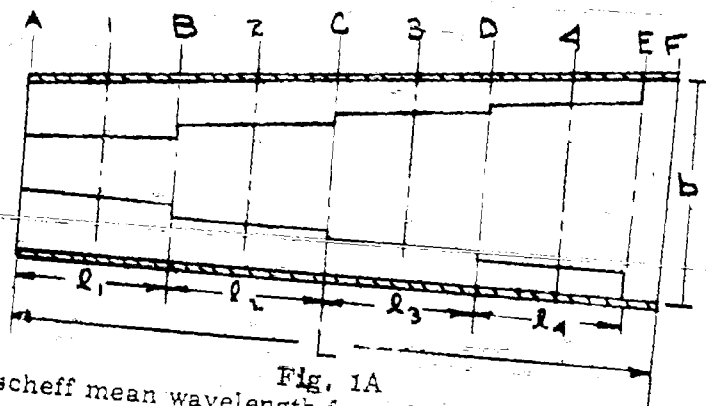
⁵ See Reference 7

$$\begin{aligned}
 Z_1 &= Z_{\text{rect.}} (Z_1')^{-\gamma_1'} = (397.2)(1.0549)^{-1} = 376.5 \\
 Z_2 &= Z_1 (Z_1')^{-\gamma_2'} = (376.5)(1.0549)^{-3.001} = 320.7 \\
 Z_3 &= Z_2 (Z_1')^{-\gamma_3'} = (320.7)(1.0549)^{-4.127} = 257.2 \\
 Z_4 &= Z_3 (Z_1')^{-\gamma_4'} = (257.2)(1.0549)^{-3.001} = 219.0 \\
 Z_5 &= Z_{\text{ridge}} = Z_4 (Z_1')^{-\gamma_5'} = (219.0)(1.0549)^{-1} = 207.6
 \end{aligned}$$

The last step is a check upon the Tchebyscheff coefficients. The final calculated impedance is sufficiently close to the actual impedance.

Figure 1A gives the overall longitudinal cross section of a typical transition.

At A
 Double Ridge
 $a = 0.471$
 $b = 0.219$
 $b/a = 0.465$
 $\lambda_c = 1.207$
 $Z_0 = 207.6$



At F
 RG-58/U
 $a = 0.420$
 $b = 0.170$
 $b/a = 0.404$
 $\lambda_c = 0.840$
 $Z_0 = 397.2$

Fig. 1A
 The Tchebyscheff mean wavelength for a frequency band is

$$\lambda_{g \text{ mean}} = \frac{2 \lambda_{gH} \lambda_{gL}}{\lambda_{gH} + \lambda_{gL}}$$

λ_{gL} = guide wavelength low frequency

λ_{gH} = guide wavelength high frequency

The mean wavelength for RG-53/U over the 18.0 to 26.5 Gc range is 0.700, while the mean wavelength in ridge guide over the same band is 0.594. Apply the formula above to get a mean mean value

$$\lambda_{g \text{ mean mean}} = \frac{2(0.594)(0.700)}{(0.594 + 0.700)} = 0.6427$$

$$\lambda_{g \text{ average}} = \frac{0.594 + 0.700}{2} = 0.6470$$

$$\lambda_{g \text{ mean average}} = \frac{0.6470 + 0.6427}{2} = 0.6448 = L$$

The mean average λ_g is used to determine the length of the first quarter wave section. From Figure 1A one can equate the "a" and "b" dimension as

$$a = a_0 + \left(\frac{\Delta a}{L}\right) x = a_0 + .0791 x$$

$$b = b_0 + \left(\frac{\Delta b}{L}\right) x = b_0 + .0760 x$$

Δa and Δb are differences in a and b dimensions from ridge to rectangular guide

First Step:

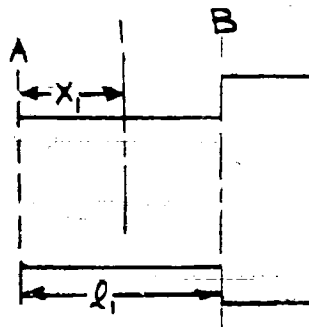


Fig. 2A

Given: At A: $a = 0.471$ in., $b = 0.219$ in.,

At x_1 : $Z_0 = 219.0 \Omega$, $\lambda_0 = 0.5378$ in. (Midband)

$$\text{Let } x_1 = \frac{L}{8} = \frac{0.6449}{8} = 0.0806 \text{ in.}$$

$$a_{x_1} = a_A + \left(\frac{\Delta a}{L}\right) x_1 = a_A + .0791x_1 = 0.4646 \text{ in.}$$

$$b_{x_1} = b_A + \left(\frac{\Delta b}{L}\right) x_1 = b_A + .0760x_1 = 0.2129 \text{ in.}$$

at x_1 : $b/a = 0.458$

let $Z_{0\infty} = 195.0$ for $b/a = 0.458$

$Z_{0\infty}$ is proportional to b/a assuming all other physical parameters are held constant.

$$\therefore Z_{0\infty} = 195.0 \left(\frac{0.465}{0.458}\right) = 198.0 \text{ for } b/a = 0.465$$

Using Figure 3A for $b/a = 0.465$, $d/b = 0.480$. This d/b will give a $Z_{0\infty}$ of 195.0 ohms for $b/a = 0.458$ within 1.5%.

Using Figure 4A with the appropriate correction factor determined from Figure 5A λ_c/a may be found to be 2.62.

$$\therefore \lambda_c = 1.217; \lambda_c/\lambda_0 = 2.263$$

$$\lambda_g/\lambda = Z_0/Z_{0\infty} = 1.12; \lambda_g = 0.6023; Z_0 = 218.4 \approx 219$$

$$d = .1022$$

$$\ell_1 = 0.245 \lambda_g \text{ (corrected for step capacitance)} = 0.1476$$

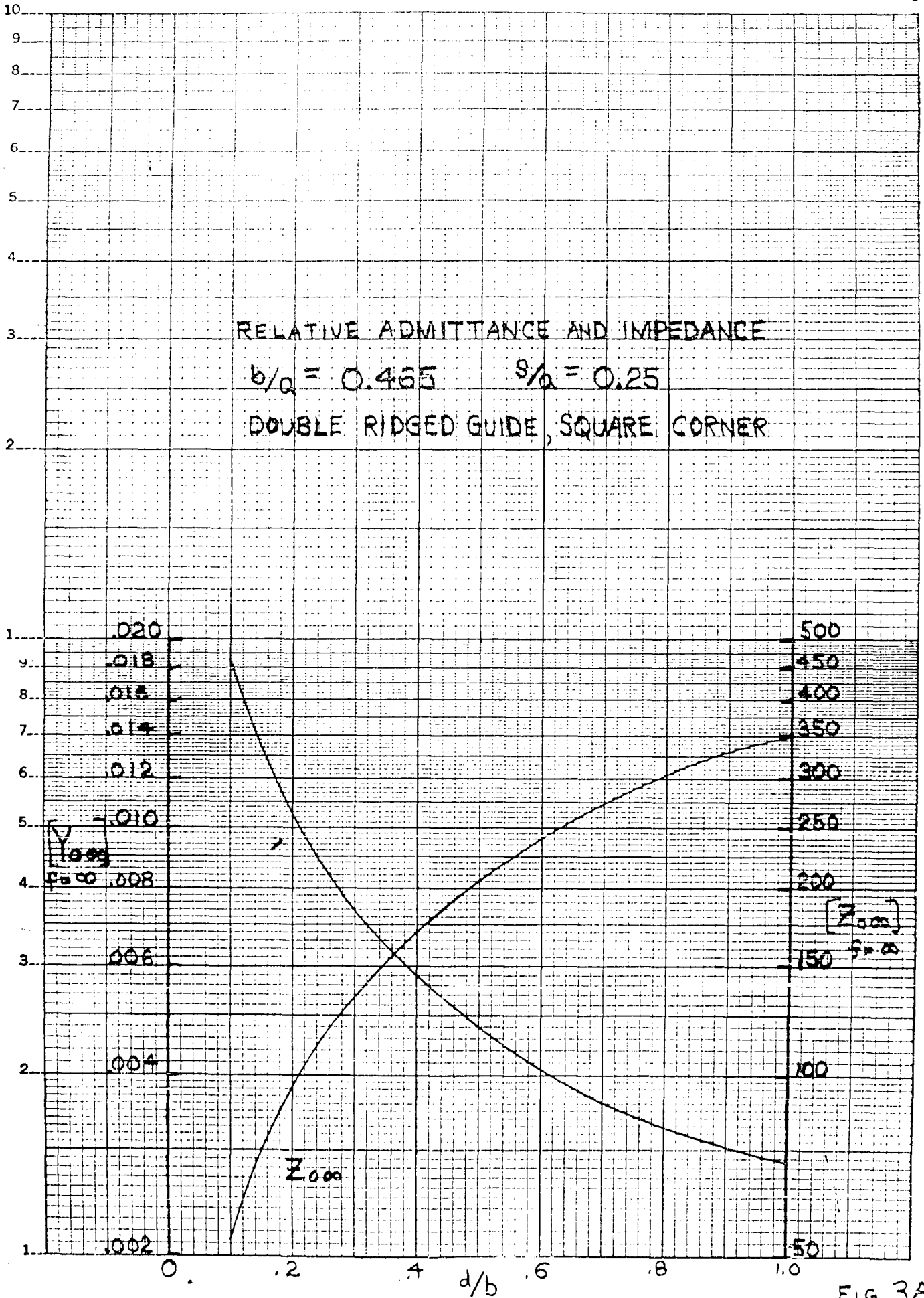


FIG 3A

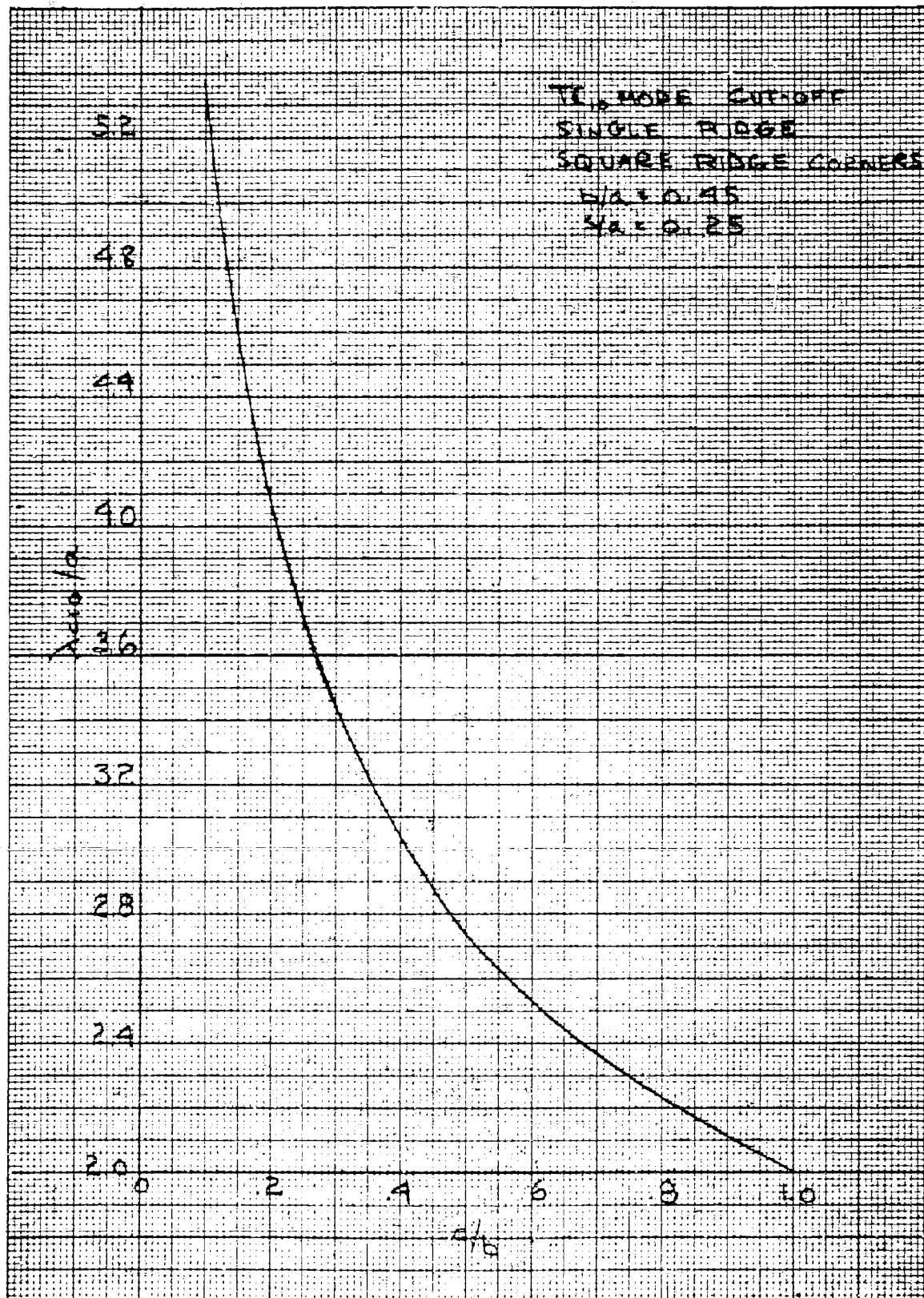


FIG. 4A

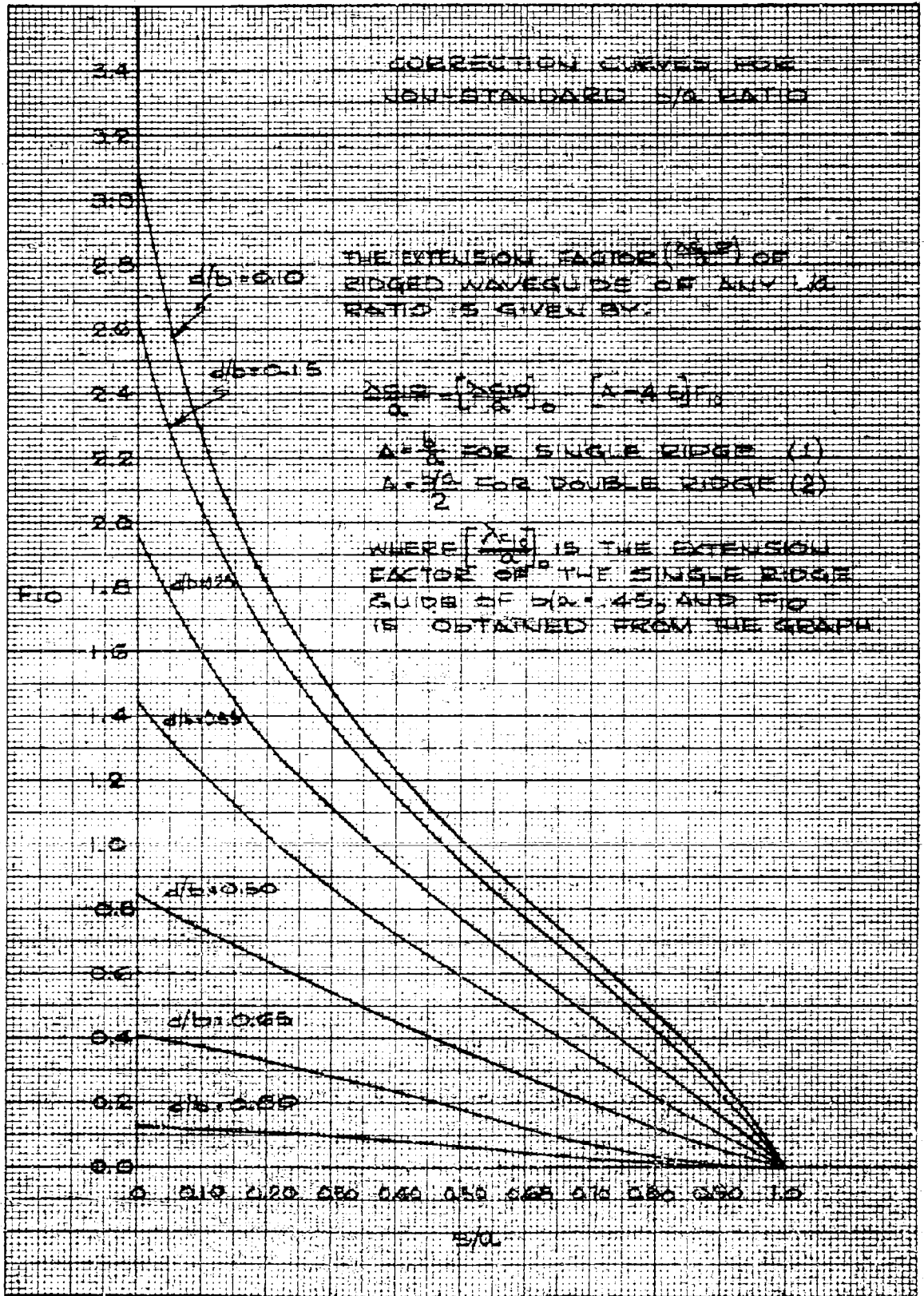


FIG 5A

If the Z_0 were not close to the required value a new Z_0 would have to be chosen and the calculation repeated until the correct value was obtained.

The parameters at point "A" are determined in the same manner, which will uniquely determine the parameters at point "B".

This process is continued until all the steps are calculated. The resultant transition gave a VSWR of 1.08 maximum.

APPENDIX B
DIRECTIONAL COUPLER DESIGN PROCEDURE

In conventional waveguide directional couplers an optimum design⁶ exists with respect to the frequency variation of coupling and the greatest minimum directivity for a given bandwidth. As the bandwidth increases the performance degenerates. The ridge guide directional coupler presents a particularly difficult design problem because of its large range of operation.

The first important consideration of the ridge guide directional coupler is the position of the coupling elements necessary to give the minimum frequency variation of coupling. A hole, the most convenient coupling element is placed in the common wall between the two adjoining waveguides.

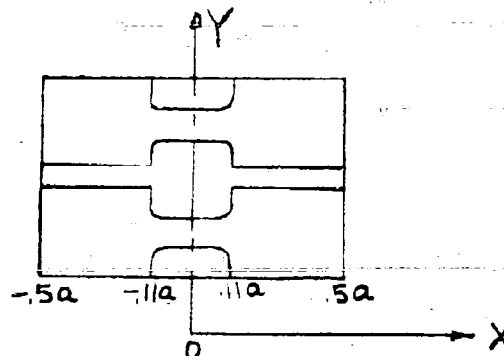


Fig. 1B

The voltage coupling of the lowest mode wave travelling in the +Z direction of the auxiliary line (Figure 1B) when excited by a wave of unit amplitude travelling in the +Z direction of the main line⁷ is

⁶See Reference 7.

⁷See Reference 11.

$$A = \frac{j\pi}{\lambda_0 Sa} (PE_{my} E_{ay} - M_1 H_{mx} H_{ax} - M_2 H_{mz} H_{az}) \quad (1)$$

E_{my} is the magnitude of the y component of the unit electric field in the main guide evaluated at the center of the aperture; E_{ay} is the same, except that it is evaluated for unit field in the auxiliary guide. Similar definitions hold for H_{mx} , H_{ax} , H_{az} and H_{mz} . P , M_1 and M_2 are positive real numbers called respectively, the electric and magnetic polarizabilities and are given by:

$$M_1 = M_2 = 2P = 4/3 r^3 \text{ for a round hole} \quad (2)$$

where r is the radius of the coupling hole. Sa is a normalizing factor given by:

$$Sa = \int_A \mathbf{E} \times \mathbf{H} \cdot d\mathbf{s} \quad (3)$$

In conforming with Bethe's notation, the field distribution for the TE_{10} mode in ridge waveguide is approximately:

$$\left. \begin{aligned} E_y &= -V_0 \cos \frac{2\pi x}{\lambda_c} \\ H_x &= V_0 \frac{\lambda}{\lambda_g} \cos \frac{2\pi x}{\lambda_c} \\ H_z &= -V_0 \frac{\lambda}{\lambda_c} \sin \frac{2\pi x}{\lambda_c} \end{aligned} \right\} 0 \leq x \leq .11a$$

$$\left. \begin{aligned} E_y &= -V_1 \sin \frac{2\pi}{\lambda_c} \left(\frac{a}{2} - x \right) \\ H_x &= V_1 \frac{\lambda}{\lambda_g} \sin \frac{2\pi}{\lambda_c} \left(\frac{a}{2} - x \right) \\ H_z &= -V_1 \frac{\lambda}{\lambda_c} \cos \frac{2\pi}{\lambda_c} \left(\frac{a}{2} - x \right) \end{aligned} \right\} .11a \leq x \leq .5a \quad (4)$$

For the operating bandwidth of 2.4 to 1 in the ridged guide waveguide V_1/V_0 is approximately 0.17. The normalizing factor Sa can be expressed as $\frac{\lambda_0}{\lambda_g} K$ where K depends upon the maximum voltage ampli-

tude and dimensions of the waveguide. Therefore the coupling in the ridged portion of the guide can be written as:

$$A = K_0 \frac{\lambda_g}{\lambda_0} \left\{ \left[4 \left(\frac{\lambda_0}{\lambda_c} \right)^2 - 1 \right] \cos^2 \frac{2\pi x}{\lambda_c} - 2 \left(\frac{\lambda_0}{\lambda_c} \right)^2 \right\} \quad (5)$$

and for the unridged portion

$$A = K_1 \frac{\lambda_g}{\lambda_0} \left\{ \left[4 \left(\frac{\lambda_0}{\lambda_c} \right)^2 - 1 \right] \sin^2 \frac{2\pi x}{\lambda_c} \left(\frac{a}{2} - x \right) - 2 \left(\frac{\lambda_0}{\lambda_c} \right)^2 \right\} \quad (6)$$

All non-frequency sensitive factors are contained in the K's.

From this it is seen that the frequency sensitivity of A is quite dependent upon the position x of the element.

In examining these relations it is found that the hole cannot be placed above the ridge because of large frequency variations of coupling and the restriction of the hole size to confine it to the fields within the ridge. A hole placed in the unridged portion of the guide at $X = .153a$ gives an approximate theoretical optimum variation of coupling of ± 3.3 db. Actually this position is found to be intolerable because for the coupling values required the holes are large enough to intersect the fields over the ridge. Experimentally, the optimum position measured is $X = .303a$, which gives a coupling variation of ± 3.55 db. The discrepancy between the theoretical and actual optimum position is primarily due to the holes being a little large for Bethe's theory to strictly apply, the field distribution of (4) not accounting for the fringing fields or the ridge edges, and the reactive attenuation through the holes not being accounted for in (6).

The next consideration in the design of the directional coupler is to attain the greatest minimum directivity for the shortest length of the coupling array. The optimum distribution makes use of the Tchebyscheff polynomial. In order to obtain a minimum directivity of 40 db, a symmetrical 14-element array is required. Voltage coupling coefficients for the holes are found from a step by step solution of⁸

$$\alpha' (N+1-q) = \frac{1}{A \frac{2q-1}{2q-1}} \left(A \frac{2N-1}{2q-1} Z_0^{2q-2N} \sum_{k=q+1}^N \alpha' (N+1-k) A \frac{2k-1}{2q-1} \right) \quad (q = N, \dots, 1) \quad (7)$$

where $2N$ is the number of elements, $\alpha' (N+1-q)$ is the coupling coefficient of the $(N+1-q)^{\text{th}}$ element relative to α_1 of the first element. Z_0 is a scale factor which is given by:

$$Z_0 = \sec \frac{\pi}{1 + \frac{\lambda_g \text{ at } 11.0 \text{ Gc}}{\lambda_g \text{ at } 26.5 \text{ Gc}}} \quad (8)$$

$$\text{and } A \frac{2k+1}{2m+1} = (-1)^{k-m} \sum_{p=k-m}^k \binom{p}{p-k+m} \binom{2k+1}{2p} \quad (9)$$

$$\text{where } \binom{n}{k} = \frac{n!}{k!(n-k)!} \quad (10)$$

⁸See Reference 7

After finding the relative coupling coefficients the following table can be made:

TABLE I

k	1	2	3	4	5	6	7
γ_k'	1	4.211	11.033	21.802	34.998	47.292	54.766
Coupling (db) Below largest hole	34.772	22.280	13.918	8.000	3.890	1.274	0
Abs. Coupling (db) for 20 db	76.888	64.396	56.034	50.116	46.006	43.390	42.116
Diam. (In.)	0.055	0.082	0.111	0.136	0.147	0.157	0.161

The absolute coupling of the largest hole is determined from:

$$C = 20 \log_{10} \left[2 \sum_{k=1}^6 \alpha_k + \kappa/\alpha_L \right] + C_0 + 6 \text{ db} \quad (11)$$

C_0 is the overall coupling array required and the 6 db is the additional coupling due to a second parallel array that is used. The diameter of the holes are found by taking coupling data as shown in Figure 37. The distance between holes is 0.1925 inches. The overall coupling results are shown in Figure 38. The average coupling is 19.85 db with a 3.55 db variation with frequency. Directivity is found to be greater than 29 db over the entire range from 11.0 to 26.5 Gc.

UNITED STATES ARMY SIGNAL RESEARCH & DEVELOPMENT AGENCY
STANDARD DISTRIBUTION
RESEARCH AND DEVELOPMENT CONTRACT REPORTS

Copies

- 1 Technical Library, OASD (R&E) Rm 3E1065, The Pentagon, Washington 25, D.C.
1 Commanding Officer, U.S. Army Signal Research and Development Agency,
Fort Monmouth, N. J., ATTN: SIGRA/SL-DE
1 Commanding Officer, U.S. Army Signal Research and Development Agency,
Fort Monmouth, N. J., ATTN: SIGRA/SL-ADT
1 Commanding Officer, U.S. Army Signal Research and Development Agency,
Fort Monmouth, N. J., ATTN: SIGRA/SL-ADJ (MF&R Unit No. 1, EC Dept.)
3 Commanding Officer, U.S. Army Signal Research and Development Agency,
Fort Monmouth, N. J., ATTN: SIGRA/SL-TN
(FOR RETRANSMITTAL TO ACCREDITED BRITISH AND CANADIAN GOVERNMENT REPS.)
3 Commanding Officer, U.S. Army Signal Research and Development Agency,
Fort Monmouth, N. J., ATTN: SIGRA/SL-LNF
1 Commanding Officer, U. S. Army Signal Equipment Support Agency,
Fort Monmouth, N.J., ATTN: SIGMS/ADJ
1 Commanding Officer, U.S. Army Signal Equipment Support Agency,
Fort Monmouth, N. J., ATTN: SIGMS/SDM
1 Director, U. S. Naval Research Laboratory, Washington 25, D.C. ATTN:
Code 2027
1 Commanding Officer and Director, U.S. Navy Electronics Laboratory,
San Diego 52, California
2 U.S. Army Signal Liaison Office, ASD-9, Wright Aeronautical Systems
Command, Building 50, Room 025, Wright Patterson Air Force Base, Ohio
1 Commander, Air Force Command and Control Development Division, Air
Research and Development Command, United States Air Force, L. G. Hanscom
Field, Bedford, Massachusetts, ATTN: CROTLR-2
1 Commander, Rome Air Development Center, Air Research and Development
Command, ATTN: RCSSLD, Griffis Air Force Base, New York
10 Commander, Armed Services Technical Information Agency, Arlington Hall
Station, Arlington 12, Virginia
1 Commanding General, Army Ordnance Missile Command Signal Office, Redstone
Arsenal, Alabama
1 Chief, Bureau of Ships, Dept. of the Navy, Washington 25, D. C.
ATTN: 691B2C
1 Commander, New York Naval Shipyard, Materials Laboratory, Brooklyn,
New York ATTN: Code 910-d
1 Commanding Officer, Diamond Ordnance Fuze Laboratories, Washington 25,
D. C., ATTN: Technical Reference Section, ORDTL-06.33
1 Commanding Officer, Engineering R&D Laboratories, Fort Belvoir,
Virginia, ATTN: Technical Documents Center
2 Chief, U.S. Army Security Agency, Arlington Hall Station, Arlington 21,
Virginia
1 Deputy President, U. S. Army Security Agency Board, Arlington Hall
Station, Arlington 12, Virginia
1 Marine Corps Liaison Officer, U.S. Army Signal Research & Development
Lab., Ft. Monmouth, N. J., ATTN: SIGRA/SL-LNR
2 Advisory Group on Electron Devices, 346 Broadway, New York 13, New York

39

SUPPLEMENTAL DISTRIBUTION

- 1 Commander, Rome Air Development Center, Griffiss Air Force Base,
New York, ATTN: RCLRA-2 (Mr. P. A. Romanelli)
Commanding Officer, U.S. Army Signal Research & Development Agency,
Fort Monmouth, N. J.
1 ATTN: SIGRA/SL-SRA (Mr. B. Gelernter)
1 ATTN: SIGRA/SL-SEA (Mr. A. DiGiacomo)
* ATTN: SIGRA/SL-PEE (Mr. L. E. Moore)
* Remaining Copies